SEP 25 1947

Registered No. M 3121

PROCEEDINGS

OF THE

INDIAN ACADEMY

OF SCIENCES

VOL. XXV] *SECTION A* [No. 3

MARCH, 1947

Price Rs. 2 or 3 Sh. *Annual Subscription Rs. 18*

PRINTED AT THE BANGALORE PRESS, BANGALORE CITY, BY G. SRINIVASA RAO, SUPERINTENDENT, AND PUBLISHED BY THE INDIAN ACADEMY OF SCIENCES, BANGALORE.

HYSTERESIS IN SORPTION

XV. Hysteresis in the Sorption of Water on Casein, Egg Albumin and Gelatin

By G. N. Subba Rao,* K. Subba Rao‡ and B. Sanjiva Rao,§ F.A.Sc.
(*Department of Chemistry, Central College, Bangalore, S. India*)

Received January 6, 1947

Introduction

Some years ago, the problem of hysteresis in sorption appeared to be inexplicable. Recent investigations on this phenomenon in this laboratory, have conclusively shown the phenomenon to be real and reproducible.[2, 3, 4] Moreover, the interesting phenomena of drift of the hysteresis loop[6] and disappearance of the hysteresis loop[7] have been discovered. It has also been shown that the cavity concept is the general explanation of the hysteresis effect and the various phenomena connected with it. In the light of the cavity concept the phenomenon of the disappearance of the hysteresis effect initially exhibited by the elastic gels has been attributed to the property of the swelling of such gels in solvating liquids. The importance of the elasticity of gels which swell on the imbibition of solvating liquids has been shown by studies in sorption on organo gels such as rice (a monocot),[3, 7] dhal (a dicot)[7] and gum arabic (a plant exudate).[9] The generality of the phenomenon has been established by further work on the sorption of water on certain proteins such as casein, egg albumin and gelatin presented in this paper.

Experimental

The McBain-Bakr quartz fibre spring technique[1] described in an earlier paper[2] was used in the present investigations.

Proteins

Casein.—Kahlbaum's "casein nach Hammersten" was employed.

Denatured casein.—Hammersten casein was treated with boiling absolute alcohol for one hour and dried in an air oven at 75° C. for one and half hours. The product obtained was found to be insoluble in aqueous sodium acetate (the original casein was soluble) but soluble in alkali.

* Government of India Scholar, Torry Research Station, Aberdeen, Scotland.
‡ Senior Research Fellow of the National Institute of Sciences of India.
§ Principal and Professor of Chemistry, Central College.

Egg albumin.—Merck's "soluble egg albumin" was employed.

Denatured egg albumin.—A solution of egg albumin (about 10%) in water was heated for one hour on a boiling water-bath, to denature the protein. The precipitated albumin was filtered, washed with water and dried at 40° C. for 2 hours in vacuum.

Gelatin lumps.—A 20% solution of gelatin (Merck's gold label) in boiling water was allowed to set in a test-tube. The gel was removed by plunging the tube in boiling water for a few seconds and suddenly inverting it. The cylindrical piece of gelatin was cut into lumps (approximately a cm. cube). These were dried slowly at room temperature in partial vacuum (about 10 cm. pressure) for 4 days.

Dehydration of proteins

In the case of casein and egg albumin, particles passing through 20-mesh and retained by 30-mesh sieves were used. When particles of this size were not available (*e.g.*, Kahlbaum's sample of Hammersten casein), the fine powder was made into a thick paste, dried in vacuum for two hours at the temperature of dehydration. The mass obtained was then ground and particles of the above-mentioned size selected.

Dehydration of each protein was effected by heating to an appropriate temperature in vacuum for six hours. The temperature of dehydration was 60° C. in the case of normal and denatured casein and 40° C. in the case of normal and denatured egg albumin.

In the case of the gelatin lump, the dehydration was effected at the temperature of the thermostat (30° C.).

Air-free water

Distilled water was kept in the bulb attached to the sorption tube and the air was flushed out in vacuum for half an hour.

Air-free ethyl alcohol

Ethyl alcohol was obtained by distilling absolute alcohol twice over metallic calcium in an all-glass distillation apparatus. The bulb was almost filled with alcohol and the air in the bulb was flushed out by allowing a portion of alcohol to evaporate in vacuum. During sorption and desorption measurements, the possibility of the grease on the stopcock being removed by the solvent action of alcohol was avoided in the same way as described for carbon tetrachloride.[5]

Sorption and desorption of water vapour

A suitable amount of the dehydrated protein was placed in the bucket attached to the spring and was degassed for 5 hours at 10^{-2} mm. attained by means of Cenco Hyvac pump. After degassing, a series of sorptions and desorptions of the vapour of liquid on the protein at 30° C. were conducted. In all the experiments sufficient time was allowed for the attainment of equilibrium. With water, about 10 hours were found to be necessary for securing equilibrium and with ethyl alcohol only one hour.

Results

Sorption of water

Casein-water.—Casein takes at the end of the 1st, 2nd and 3rd sorptions, 33·0 gm. 33·6 gm. and 37·4 gm. of water respectively per 100 gm. at saturation pressure. The initial hysteresis loop is reduced in size in the 2nd cycle of sorption and desorption and entirely disappears in the 3rd (Fig. 1).

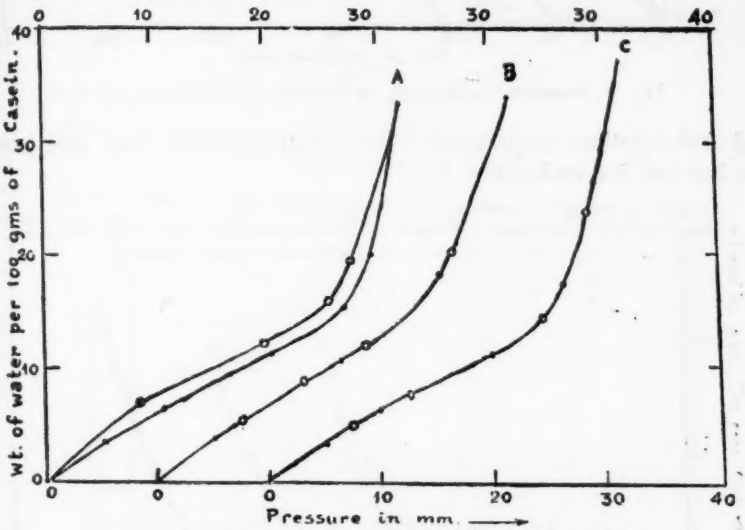

Fig. 1. Casein-water (A 1st cycle, B 2nd cycle, C 3rd cycle)

Denatured casein-water.—The sorptive capacity of denatured casein for water, at the end of the three successive sorptions are 32·7 gm., 34·0 gm. and 34·3 gm. of water respectively per 100 gm. The hysteresis loop obtained in the first cycle disappears in the subsequent cycles, Fig. 2.

Egg albumin-water.—Egg albumin takes at saturation pressure, 62·8 gm., 68·8 gm. and 81·2 gm. of water per 100 gm. at the end of the 1st, 2nd

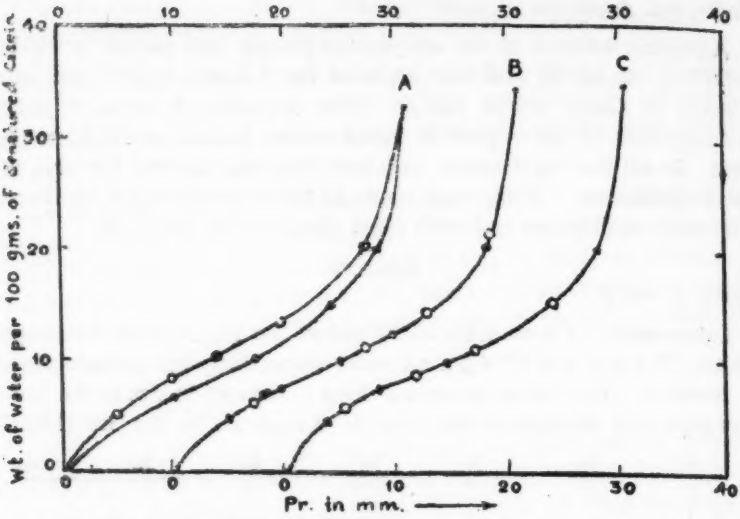

FIG. 2. Denatured casein-water (A 1st cycle, B 2nd cycle, C 3rd cycle)

and 3rd sorptions respectively. The initial hysteresis loop disappears in the 2nd and 3rd cycles (Fig. 3).

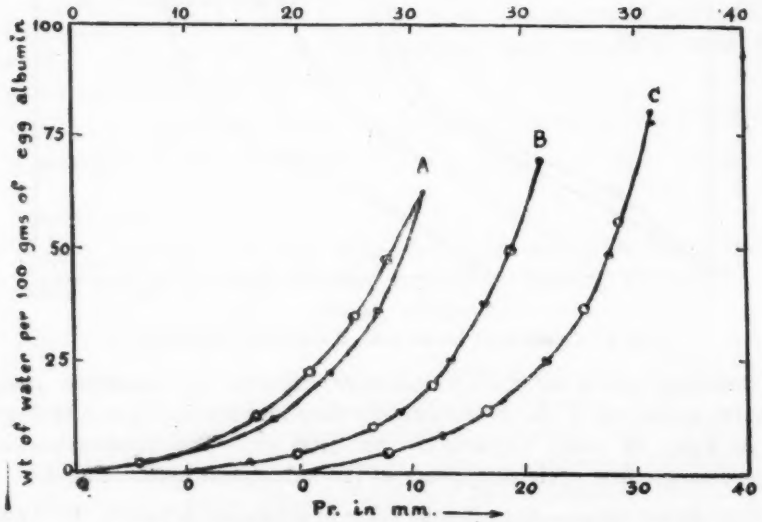

FIG. 3. Egg albumin-water (A 1st cycle, B 2nd cycle, C 3rd cycle)

Denatured egg albumin-water.—The sorptive capacities in the 1st, 2nd and 3rd cycles are 38·4 gm. 45·6 gm. and 47·4 gm. per 100 gm. of the denatured protein. There is no hysteresis loop at all even in the 1st cycle (Fig. 4).

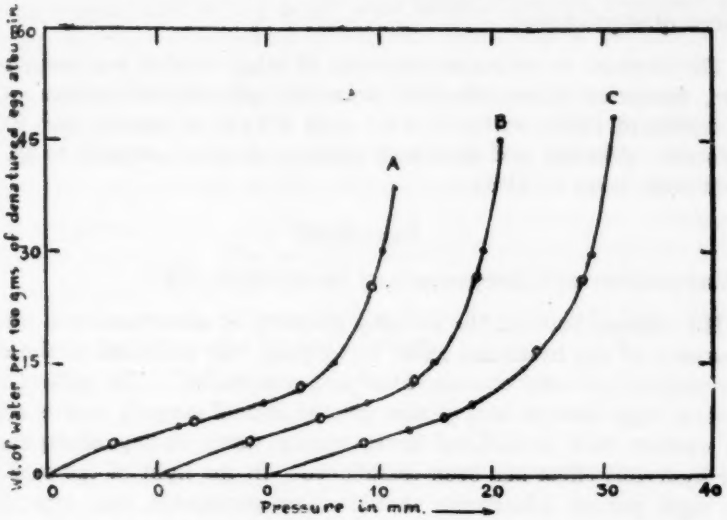

FIG. 4. Denatured egg albumin-water (A 1st cycle, B 2nd cycle, C 3rd cycle)

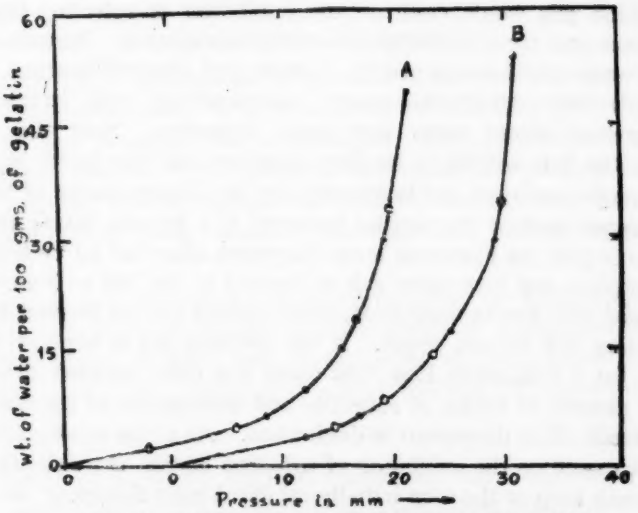

FIG. 5. Gelatin lump-water (A 1st cycle, B 2nd cycle)

Gelatin lump-water.—Sorptive capacities at saturation pressure at the end of the 1st and 2nd sorptions are 48·7 gm. and 55·4 gm. per 100 gm. There is no hysteresis loop even in the 1st cycle (Fig. 5).

Sorption of ethyl alcohol

The sorption at saturation pressure of ethyl alcohol was measured on casein, denatured casein, albumin, denatured albumin and gelatin. Casein and denatured casein sorbed 1·8 c.c. and 9·9 c.c. of alcohol per 100 gm. of protein. Albumin and denatured albumin show no sorption at all. The gelatin lump takes no alcohol.

Discussion

Swelling property and disappearance of the hysteresis effect

The relation between the swelling property of adsorbents and the disappearance of the hysteresis effect in sorption was indicated in the studies in the sorption of water on rice,[8] dhal[7] and gum arabic.[9] The present studies on casein, egg albumin and gelatin give additional support to this relation. That cavities with constricted necks entrap water during desorption and cause hysteresis effect has been established. In the light of the cavity concept, rigid porous adsorbents should show permanent and reproducible hysteresis effect on successive sorptions and desorptions and instances of remarkable permanence and reproducibility have already been recorded.[2, 4] With elastic gels which swell on the imbibition of solvating liquids, such permanence and reproducibility are not to be expected. Proteins in general swell in water and become elastic. Casein and albumin (normal as well as denatured) when dehydrated have a comparatively rigid structure. Their stable cavities entrap water and cause hysteresis. Near the saturation pressure, the gels will be in swollen condition and the cavity walls elastic. At this stage conditions are favourable for the disappearance of the cavities. The disappearance of the cavities however, is a process taking time. With some elastic gels the hysteresis loop disappears after the 1st cycle of sorption and desorption and with other gels at the end of the 2nd or 3rd cycle. It is to be noted that during desorption, fresh cavities are not formed but cavities still existing will remain intact. If the swelling gel is kept at saturation pressure for a sufficiently long time (days and even months), it is probable that the number of cycles of sorptions and desorptions at the end of which the hysteresis effect disappears is diminished. As a rule in all elastic adsorbents which swell on the imbibition of solvating liquids, there should be either no hysteresis loop or the loop initially exhibited must disappear on successive sorptions and desorptions. With nonsolvating liquids however there should

be permanent and reproducible hysteresis effect. This is illustrated in rice-carbon tetrachloride system.[7]

The observations on the gelatin lump are of great interest. In this adsorption experiment with a single solid lump of gelatin, free from pores, no hysteresis effect was noticed in the very first cycle of sorption and desorption. This is to be expected on the basis of the cavity concept. Denatured albumin behaves similarly, showing no hysteresis loop in the first cycle though it was activated at the same temperature (40° C.) as the normal albumin. Either cavities have all collapsed during denaturation or fresh cavities are not produced during dehydration, of the denatured protein.

Experiments on the sorption of ethyl alcohol on casein, albumin and gelatin are interesting. The sorptive capacity is negligibly small. Alcohol is a nonsolvating liquid for casein, albumin and gelatin and there is no swelling in this liquid. Consequently sorption is very low with casein and there is no sorption at all with egg albumin.

Another feature is the progressive increase in the sorptive capacity for water of the proteins on successive sorptions and desorptions. Gelatin, normal and denatured casein and albumin exhibit this property. Such a behaviour has been noticed in rice, dhal and gum arabic and is attributed to the loosening of the gel structure.

Denaturation and Sorptive Capacity

The sorptive capacities of denatured casein and denatured albumin are lower than those of normal casein and albumin.

The subject of denaturation of proteins has attracted considerable attention during recent years. It is a well-known fact that proteins undergo change in their properties on denaturation. They become less soluble and their swelling gets less. It is probable that on denaturation, casein and egg albumin become less hydrophilic and swell in water to a smaller extent and consequently have lower sorptive capacities than normal casein and egg albumin.

The high sorptive capacity of denatured casein for ethyl alcohol (9·9 c.c. per 100 gm.) in comparison with the low value for normal casein (1·8 c.c. per 100 gm.) also indicates that on denaturation the proteins become less hydrophilic and show a tendency to adsorb more of the nonsolvating liquids.

Summary

A series of sorptions and desorptions of water vapour at 30° C., on gelatin, casein, egg albumin, denatured casein, denatured egg albumin have

been conducted and in these systems either there is no hysteresis loop at all or the loop initially exhibited disappears on successive sorptions and desorptions.

These results indicate that the swelling of the adsorbent on imbibing the solvating liquid is responsible for the disappearance of the hysteresis effect.

Experiments on the sorption of ethyl alcohol at saturation pressure on the above proteins at 30°C. show that the nonsolvating liquid is either not adsorbed at all or taken up to a very small extent.

With casein and egg albumin, the sorptive capacities for water are lower in the denatured forms of the proteins. These results indicate a decrease in hydrophilic character of the proteins on denaturation.

References

1. McBain and Bakr .. *J. Am. Chem. Soc.*, 1926, **48**, 696.
2. Rao, K. S. .. *J. Phys. Chem.*, 1941, **45**, 500.
3. ———— .. *Current Science*, 1939, **8**, 256.
4. ———— .. *J. Phys. Chem.*, 1941, **45**, 506.
5. ———— .. *Ibid.*, 1941, **45**, 517.
6. ———— .. *Ibid.*, 1941, **45**, 522.
7. ———— .. *Ibid.*, 1941, **45**, 531.
8. ———— .. *Current Science*, 1939, **8**, 256.
9. ———— .. *Ibid.*, 1940, **9**, 19.

HYSTERESIS IN SORPTION

XVI. Sorption of Water on Some Indian Soils and Soil Fractions

By Miss Sharda Gulvady,* K. Subba Rao‡ and B. Sanjiva Rao,§ F.A.Sc.
(Department of Chemistry, Central College, Bangalore, S. India)

Received January 6, 1947

Introduction

The problem of retention of moisture by soils has been extensively studied by numerous workers. Recent investigations on the phenomenon of Hysteresis in sorption[3] have thrown much light on the porous structure of rigid and elastic adsorbents. With a view to investigate the porous structure of soils, a study of hysteresis was undertaken with reference to the sorption of water on a red laterite soil and black cotton soil and on the clay, silt and fine sand fractions of the soils. The decrease in sorptive capacity of the soils on the removal of organic matter has been studied.

Experimental

Mechanical analysis of soils.—According to the International Society of Soil Science, soil passing through a 2 mm. sieve called "Fine earth" is divided into the following four fractions—coarse sand (2–0·2 mm.), fine sand (0·2–0·02 mm.), silt (0·02–0·002 mm.) and clay (less than 0·002 mm.). The international method A was employed for resolving the soil into these fractions.[9] In place of ammonia, sodium hydroxide was used as the dispersing agent.

Estimation of organic matter in the soil.—For the estimation of organic matter in the soil, the new modified volumetric method using chromic acid[6,7,8] was adopted. The results of the mechanical analysis of the two soils are given in Table I. The accuracy of the method is 2%.

Activation of the soil and soil fractions.—Soil particles passing through 20-mesh sieve but retained by 30-mesh sieve were used. In the case of soil fractions, the dry powder passing through 100-mesh sieve was used. The samples were activated by heating to 80° C. for 6 hours in vacuum obtained by the Cenco hyvac pump.

---

* Research Scholar, Indian Institute of Science, Bangalore.
‡ Senior Research Fellow of the National Institute of Sciences of India.
§ Principal and Professor of Chemistry, Central College.

TABLE I

Mechanical fractions	Fractions of red soil per 100 gm. soil	Fractions of black cotton soil per 100 gm. soil
	gm.	gm.
Coarse sand ..	40·6	5·2
Fine sand ..	22·6	45·5
Silt ..	2·9	15·5
Clay ..	30·7	33·9
Organic matter ..	0·25	0·63

Sorption and desorption of water vapour.—The quartz fibre spring technique[8] was employed in the study of sorptions and desorptions of water vapour on the soils and soil fractions. A suitable amount of the activated adsorbent was placed in the bucket. The adsorbent was degassed by evacuation for 6 hours at 10^{-2} mm. A series of sorptions and desorptions of water vapour at 30° C. was conducted. The results are indicated in Figs. 1 and 2.

The sorptive capacities (for water vapour at saturation pressure) of red laterite soil and black cotton soil before and after treatment with

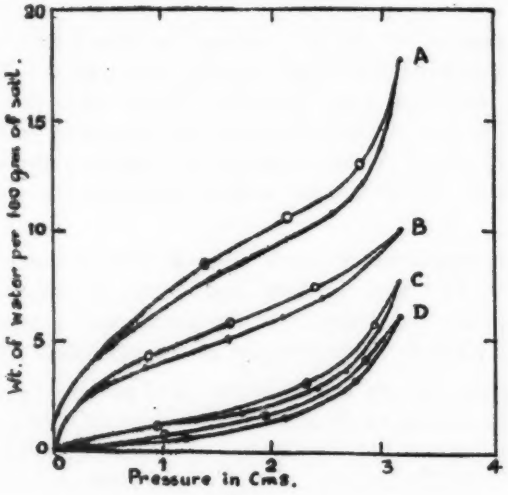

FIG. 1

Sorption and desorption of water vapour on

A. Black cotton soil with organic matter (3rd cycle).
B. ,, ,, without organic matter (2nd cycle).
C. Red soil with organic matter (3rd cycle).
D. ,, without organic matter (2nd cycle).

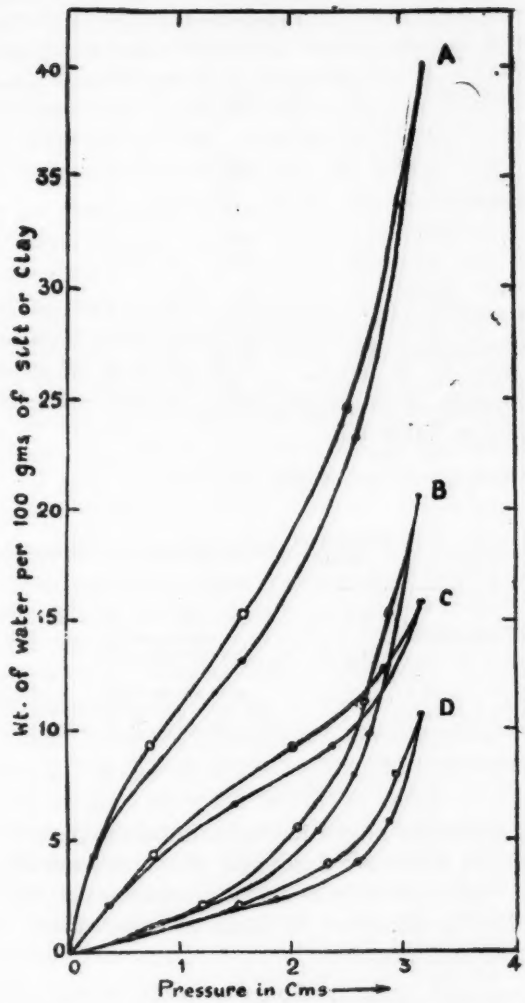

FIG. 2

Sorption and desorption of water vapour on

A. Clay from black cotton soil (2nd cycle).
B. Clay from red soil (2nd cycle).
C. Silt from black cotton soil (2nd cycle).
D. Silt from red soil (2nd cycle).

hydrogen peroxide and of their fractions—clay, silt and fine sand—are given in Table II.

TABLE II

Soil and soil fractions	Red soil. Sorption of water per 100 gm.	Black cotton soil. Sorption of water per 100 gm.
	gm.	gm.
Soil with organic matter ..	8·0	18·0
Soil without organic matter ..	6·2	9·9
Fine sand ..	0·4	0·5
Silt ..	11·2	15·8
Clay ..	21·5	40·6

From the percentage of the various fractions of the soil and their sorptive capacities for water at saturation pressure, total sorption contributed by the various fractions in 100 gm. of soil has been calculated. This in relation to the sorption of the original and hydrogen peroxide treated soils has been indicated in Table III.

TABLE III

Red soil and its fractions	Sorption of water	Black cotton soil and its fractions	Sorption of water
Red soil original ..	8·0 %	Black cotton soil original	18·0 %
Red soil treated with hydrogen peroxide ..	6·2 %	Black cotton soil treated with hydrogen peroxide	9·9 %
Fine sand (22·6 gm. at 0·4%) .. 0·09	7·02%	Fine sand (45·5 gm. at 0·5%) .. 0·23	16·44%
Silt (2·9 gm. at 11·2%) .. 0·33		Silt (15·5 gm. at 15·8%) 2·45	
Clay (30·7 gm. at 21·5%) 6·6		Clay (33·9 gm. at 40·6%) 13·76	

DISCUSSION

The sorptive capacities of red laterite soil and black cotton soil at the saturation pressure of water are 8 gm. and 18 gm. respectively per 100 gm. of activated soil. The difference in sorptive capacities is obviously due to several factors such as difference in chemical composition, soil fractions, organic matter and soil structure.

As is to be expected, removal of organic matter of the soil by treatment with hydrogen peroxide reduces the sorptive capacity of the soil for water. The red soil had 0·25% organic matter while the black cotton soil had 0·63%. On removal of organic matter, red soil suffered a decrease in sorptive capacity from 8·0% to 6·2% and black cotton soil from 18·0% to 9·9%. The effect of a given amount of organic matter on pore space seems to depend on the nature of the constituents of the soil. The exact picture of the spatial distribution of the organic matter in soils is obscure.

The sorptive capacity of fine sand is negligibly small, while that of silt is much higher. Clay has markedly higher sorptive capacity than silt. The increase in sorptive capacity from fine sand to silt and from silt to clay is more marked in the black cotton soil than in the red soil. It is noteworthy that clay from black cotton soil takes up nearly twice the amount of water sorbed by clay from the red soil. Similarly, silt from the black cotton soil takes up more water than that from red soil, Table II and Fig. 2.

Knowing the percentage of the three soil fractions—fine sand, silt and clay and their sorptive capacities it is possible to calculate the total sorption of water as contributed by the three fractions, Table III. In red soil, total sorption of water due to these fractions in 100 gm. of soil is 7·02 gm. whereas those of the original and hydrogen peroxide treated soils are 8·0% and 6·2% respectively. The total value contributed by the component fractions is intermediate between those of the original and hydrogen peroxide treated soils. In the case of the black cotton soil, the total sorption contributed by the fractions is 16·44 gm. This value is also intermediate between sorption by the original soil (18·0%) and hydrogen peroxide treated soil (9·9%).

In all the systems investigated, permanent and reproducible hysteresis loops have been obtained. This indicates that unlike elastic adsorbents like rice,[1] gum arabic,[2] and proteins,[5] the soils and their fractions are rigid porous systems, having cavities with constricted ends which are responsible for the hysteresis effect. The soils thus retain more of water during desorption than during sorption.

Soil in nature is periodically exposed to extremes of weather—very dry and highly humid. By virtue of the rigidity of its structure, a soil subjected to extremes of weather, when changed from highly humid condition to one of normal humidity retains greater amount of water than what it would hold when changed from very dry weather. This excess of water amounting to about 1% may be negligible when soil is saturated with water in highly humid weather but is appreciable in weather of normal humidity in which water holding capacity of the soil is less than half. For example at 50% humidity, red soil holds only 2% water. Compared with this, the excess 0·5% water-entrapped in the cavities is quite considerable. It is probable that the hysteresis effect exhibited by soils is of practical importance in the conservation of moisture by soils in nature.

Summary

Studies in sorption and desorption of water vapour at 30° C. on red laterite soil and black cotton soil and their fractions—fine sand, silt and

clay have been carried out. Sorptive capacity of fine sand is found to be very small. That of silt is higher. Clay fractions have the highest sorptive capacity. Removal of organic matter lessens the sorptive capacity of the soil.

The soils and their fractions have all yielded permanent and reproducible hysteresis loops. There is thus evidence that in soils we are dealing with rigid systems having cavities with constricted ends. The practical importance of the hysteresis effect in soils in nature is indicated.

References

1. Rao, K. S. .. *Current Science*, 1939, **8**, 256.
2. ———— .. *Ibid.*, 1940, **9**, 19.
3. ———— .. *J. Phys. Chem.*, 1941, **45**, 500.
4. ——— and Rao, B. S. .. *Proc. Ind. Science Congress*, 1942, **3**, 67.
5. Rao, G. N. S., Rao, K. S., and Rao, B. S. "Hysteresis in Sorption, XV," *Proc. Ind. Acad. Sci.*, 1947, **25**, 221.
6. Tiurin, I. V. .. *Pedology*, 1931, **26**, 36–37.
7. ———— .. "Genesis Cartogr Soils Dokuchaieve Soil Inst," *Acad. Sci., U.S.S.R.*, 1935, 139–58.
8. Waksman .. *Humus*, Bailliere, Tindall and Cox, London, 1936, 404–05.
9. Wright, C. H. .. *Soil Analysis, Physical and Chemical Methods*, Thomas Murby & Co., London, 1934, 33.

ULTRASONIC VELOCITY IN LIQUIDS AT HIGH FREQUENCIES

By T. Ravindranath

(From the Department of Physics, Andhra University, Waltair)

Received January 20, 1947

(Communicated by Prof. S. Bhagavantam, F.A.SC.)

1. Introduction

The problem of the dispersion of ultrasonic velocity in liquids has been investigated by Boyle and G. B. Taylor,[1] R. W. Wood, A. L. Loomis and J. C. Hubbard,[2] S. Parthasarathy,[3] Bär,[4] and K. G. Krishnan.[5] All the investigators excepting Bär worked in the range of frequencies between a few Kilocycles and 20 Megacycles per second. They observed no definite evidence of dispersion in any of the liquids studied. Bär used exceptionally high frequencies and measured velocities in water at 50 M.C. He too observed no dispersion.

In this laboratory, it has been possible to construct a V.H.F. oscillator capable of reaching 50 M.C. Refined methods of comparing ultrasonic velocities in a liquid at different frequencies are used in a fresh attack on the problem. The present paper gives the results of experiments on ultrasonic velocities in two liquids, namely, water and xylol in the ranges of frequencies 42 M.C. to 2 M.C. and 32 M.C. to 2 M.C. respectively.

2. Experimental

Water and xylol, purified by careful redistillation, are taken for investigation. The source of ultrasonics is a tourmaline plate cut in this laboratory and excited into resonant vibration at some one of its overtones by a Hartley oscillator. A specially designed Very High Frequency oscillator is used to work in the range of frequencies between 10 M.C. and 40 M.C. The circuit is the Hartley shunt-fed one with a slight modification. Filament chokes are used to isolate the circuit from external loops of wire. Connecting leads, which at lower frequencies would serve merely to join tank condenser to tank coil, have greater inductance at such high frequencies than the tank coil itself and hence they are completely avoided. Regarding the tank circuit, to develop the necessary back voltage across the tank, and thence the high anode swing, a very low tank condenser of value ·00005 is

used. A loop of copper strip 8 cm. in diameter, bridging the tank condenser serves as the tank inductance at 42 M.C. The frequency of the oscillator is measured using a reaction receiver in conjunction with a heterodyne wavemeter both of which have ranges of frequencies extending from a few K.C. to 15 M.C. At very high frequencies, using the method of autodyne reception with the reaction receiver, audible beat notes are obtained at positions of the receiver tuning, which are submultiples of oscillator frequency. The receiver being kept at one of the above places, the frequency meter is coupled to it, and a known harmonic of the frequency meter is then made to beat with the oscillator. The oscillator frequency is determined from the frequency meter reading, and a knowledge of the number of its harmonic.

The diffraction pattern is photographed on sensitive plates giving short exposures such that there is no appreciable temperature rise during the exposure. The aperture of the camera lens is cut down to less than one centimeter diameter to obtain an extremely sharp diffraction pattern. The fringe width is measured with a Hilger comparator correct to 1 to 2 parts in 10,000.

The velocities are thus determined at a number of different frequencies, the temperature in all cases being maintained the same. Results are given below from which it can be seen that there is no evidence of dispersion. The chief source of error in the comparison of velocities at different frequencies is due to the slight and unavoidable temperature difference between the two velocity measurements. In order to overcome this criticism, measurements with water are made in which ultrasonic waves of two different frequencies are produced simultaneously in the liquid by exciting the crystal at two of its harmonics with the V.H.F. oscillator and the low frequency oscillator at the same time.* The sample pictures of the diffraction pattern with simultaneous excitation are reproduced in Plate XIII and it shows the diffraction lines due to the combination and difference frequencies $n_1 + n_2$ and $n_1 - n_2$ and $n_1 - 2n_2$, where n_1 and n_2 are the oscillator frequencies. The results reveal no dispersion of ultrasonic velocity.

It may be noted here that at 42 M.C., the wavelength in water is so small that the ultrasonic grating is able to resolve clearly the full radiation from the mercury arc into its various components with a considerable dispersion. Such photographs are obtained but not reproduced here.

---

* The application of the method of simultaneous excitation to the problem of dispersion of ultrasonic velocity was first made by S. Parthasarathy and others, *Jour. Sci. and Ind. Research*, 1945, 3, 299.

Fig. 1

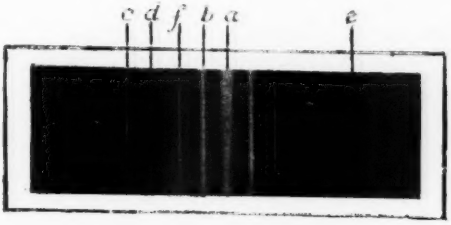

Fig. 2

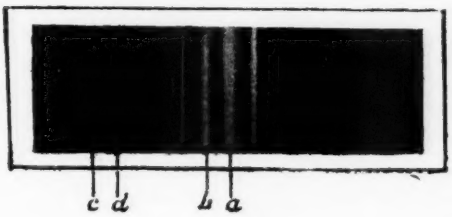

Fig. 1

a — Central line
b — 9·4 M.C. = n_2
c — 40 M.C. = n_1
d — 30·6 M.C. = $n_1 - n_2$
e — 49·4 M.C. = $n_1 + n_2$
— 21·2 M.C. = $n_1 - 2n_2$ (close to *f*)

Fig. 2

a — Central line
b — 9·4 M.C. = n_2
c — 55 M.C. = n_1
d — 45·6 M.C. = $n_1 - n_2$

TABLE I

Ultrasonic velocities in water

Temperature °C.	Frequency Megacycles per second	Velocity Meters per second
34·7	41·45	1540
34·7	16·91	1542
34·7	13·16	1540
34·7	5·639	1544
34·7	1·841	1544

TABLE II

Ultrasonic velocities in xylol

Temperature °C.	Frequency Megacycles per second	Velocity Meters per second
32·3	31·91	1311
32·3	20·67	1311
32·3	16·90	1312
32·3	9·418	1313
32·3	2·060	1314

TABLE III

Ultrasonic velocities in water: Simultaneous excitation

Temperature °C.	Frequency Megacycles per second	Velocity Meters per second
33·8	39·504	1536
	9·444	1536
33·4	39·42	1534
	13·12	1534

4. SUMMARY

Two liquids namely, water and xylol, are investigated for the ultrasonic velocity in the range from 2 M.C. to 42 M.C. and 2 M.C to 32 M.C. respectively. No evidence of dispersion is observed.

REFERENCES

1. Boyle and G. B. Taylor .. *Trans. Roy. Soc. Canada*, 1927, **21**, 79.
2. R. W. Wood, A. L. Loomis & J. C. Hubbard .. *Phil. Mag.*, 1927, **4**, 417.
3. S. Parthasarathy .. *Proc. Ind. Acad. Sci.*, 1937, **4**, 17.
4. R. Bär .. *Ibid.*, 1939, **8**, 289.
5. K. G. Krishnan .. *Ibid.*, 1939, **9**, 382.

ANISOTROPY IN THE ELASTIC BEHAVIOUR OF ROCKS

By G. H. S. V. Prasada Rao, M.Sc.

(Geology Department, Andhra University, Waltair)

Received January 23, 1947

(Communicated by Prof. S. Bhagavantam, F.A.SC.)

1. Introduction and Existing Experimental Methods

The elastic behaviour of quasi-isotropic aggregates was treated by Voigt in 1887. Bruggeman (1930) gave a theory, in which an attempt was made to treat the boundary conditions rigorously. Special aggregates consisting of two kinds of isotropic particles have also been treated by Bruggeman (1937). These theories were tested with natural crystals such as quartz, fluorite, calcite, and barite; and with aggregates of these crystals occurring in nature. Calculated values are always higher than the observed ones. Birch (1938) says, "In any particular aggregate the question of directional properties may be investigated." From this statement we can infer that he expects a directional variation in the elastic behaviour, but the methods in vogue are not powerful enough to tackle the problem.

Adams and Coker (1906), Adams and Gibson (1931), Adams and Williamson (1923), Bridgman (1924, 1925), Birch (1936), Von Karman (1911), Roess (1935) and Zisman (1933) studied the elastic behaviour of rocks by static methods. Birch and his collaborators (1937, 1938, 1940, 1943), Ide (1933, 1935, 1937), Grimme (1938), and Kausakabe (1904–05) investigated the elastic behaviour by dynamic methods. The static methods used in those investigations are the common ones such as bending, twisting and compressing under static loads, bending and twisting periodically by impact or otherwise, bouncing spheres from a polished surface, etc. Dynamic methods fall into two groups according as the measurement is made (1) by detecting the frequency at which resonance occurs when the specimen is maintained in vibration by a piezo-electric or electromagnetic driving device or by electro-static traction or (2) by direct measurement of the frequency of vibration set up by tapping or otherwise exciting free vibration. All the above methods have certain limitations. For example, static methods are known to give rise to complex creep effects or elastic hysteresis. The presence of minute cracks or other bedding planes which are either inherent in the rocks or produced in the preparation of the samples make the static method unreliable. Ide (1937) has shown that static results are always

lower than the dynamic ones by more than 10 per cent. " Due to the inherent inadequacy of the static measurements." Piezo-electric driving device requires much power and involves the complication of coupled circuits. The accuracy of the driving device is limited by the loading effect of the attached crystal.

2. Description of a New Dynamic Method

Bhagavantam and Bhimasenachar (1944) have recently developed a new method which is of importance in studying the elasticity of all solids. This method, known as the " Wedge method ", is based on the principle that a piezo-electric wedge can be made to give out an ultrasonic beam of a continuously varying frequency. This method opens up new possibilities of geophysical investigations and for the successful application of the same in determining the directional dependence of the propagation of elastic waves.

It is well known that plane parallel plates of piezo-electric crystals when used in oscillatory circuits act as generators of specified frequencies, the actual value of the frequency being dependent on the thickness of the plate. Instead, when a wedge is used, the behaviour is somewhat different on account of its varying thickness. As the exciting frequency of the electrical circuit is varied, an appropriate portion of the wedge responds to the electrical frequency and generates an ultrasonic beam of that frequency. Thus the continuously varying thickness of the wedge enables a continuous band of ultrasonic beam being obtained. The range of the band depends upon the dimensions of the wedge. The lower limit is fixed by the maximum thickness and the upper limit by the power of the driving circuit, the sensitiveness of the detecting device and the breaking stress of the crystal employed. The range of the tourmaline wedge used in these investigations is from 1 to 12 megacycles per second. For avoiding mounting effects, the area of the specimen under investigation must be larger than that of the wedge. This wedge is placed on the rock plate of known orientation. As the frequency of the electrical circuit is varied, ultrasonic energy which is of different frequencies when different regions of the wedge respond, passes through the plate. When the frequency of the wedge in a particular position coincides with a natural frequency or an overtone thereof of the rock section, the latter begins to resonate.

The rock section and the wedge are mounted in a special holder consisting of an annular brass plate electrode secured by a brass rod to an ebonite plate. The rock plate of uniform thickness is placed on this electrode. The wedge is laid on the specimen with a film of oil in between to facilitate good acoustical contact. On the top of the wedge a small brass disc is placed

and the whole arrangement is held pressed lightly against the brass plate by a fine spring. The spring acts as a second electrode. The entire set up is mounted on another ebonite plate and is provided with spring loaded levelling screws to facilitate accurate alignment. The arrangement is lowered into a rectangular cell containing carbon tetrachloride such that only the lower surface of the rock section comes into contact with the liquid. The ultrasonic beam from the wedge passes through the rock section and enters the liquid. A beam of light with the usual optical arrangement is allowed to pass through the ultrasonic grating set up in the liquid and the Debye-Sears diffraction patterns are observed. The intensity of these patterns is a maximum when the rock section resonates. This permits the resonance position to be detected. The frequency in that position is then measured with an accurate wavemeter. On account of the neatness of the method and its decided advantage in studying even small fragments of the materials, the work is extended in the present studies to the investigation of the directional variation of the elastic behaviour of representative specimens of sedimentary and igneous rocks.

3. Description of the Specimens

A brief description of various rocks studied in these investigations is given here.

(*a*) *Sedimentary rocks*

Kurnool limestone.—The colour is steel black to bluish black. It contains disseminated specks of pyrites. It is cryptocrystalline.

Bhima limestone.—This specimen from the middle division of Bhima formation of Hyderabad state is cryptocrystalline.

Jubbalpore marble.—It is a white medium-grained marble having a pearly lustre. The individual grains of calcite show interlocking texture.

Grey Hyderabad marble.—This Pakhal marble, having a vitreous lustre, contains calcite, dolomite and tremolite.

Pink Rajaputana marble.—This fine-grained pink marble has a pearly lustre. Calcite, dolomite and quartz are the constituents.

(*b*) *Igneous rocks*

Gneiss.—(Uxbridge, U.S.A.). The crystals of hornblende are linearly arranged. Interwoven with these bands there are elongated prisms of zoisite. Quartz is present in abundance. The gneissic texture is clear.

Pink Hyderabad granite.—The colour is mottled pink, white and black due to felspars (microperthite and plagioclase) and biotite respectively. The texture is hypidiomorphic inequigranular.

Granite of Kondavidu.—It occurs as distinct entities with defined directional trends in the Kondavidu hill ranges. It is medium-grained holocrystalline rock consisting mainly of flesh red felspar and colourless blebs of quartz. Microperthite, oligoclase, muscovite and magnetite are the other constituents. The texture is hypidiomorphic and it is inequigranular.

Leptynite (from Kondavidu).—This rock is dominantly felspathic in type and is an important variety occurring along the entire range in association with charnockites and often in contact with kondalites. It is an equigranular medium grained rock having a mottled appearance due to colourless quartz blebs, pink garnets, felspars (microperthite and plagioclase) and biotite specks. The texture is xenomorphic granular.

Keratophyre (Pitshead, Snowden, North Wales).—It is a porphyritic rock with rectangular plates of white felspar with dark mafites represented by leucoxene and chlorite in a megascopically dense light coloured ground mass of white, bluish and greyish colour. The texture is porphyritic with felspathic ground mass.

Norite of Kondapalli.—It occurs as dykes and segregated bands. It is xenomorphic granular rock. Plagioclase predominates. Concentrated portions of hypersthene contain minute flakes of brass yellow mineral (Chalcopyrite ?). Diopside, magnetite and apatite are the other constituents.

Chloritised dolerite (from Hyderabad).—It is a green rock essentially composed of felspar, chlorite and augite. It is very much altered. Pyrite occurs in cubes. The augite and the altered plagioclase are intergrown in an ophitic manner.

Dunite.—(Mt. Dunn, Newzealand). It is light yellowish green on fresh surfaces and shows a greasy to glassy lustre. The texture is xenomorphic granular with predominantly olivine and chromite.

Deccan trap from Gulberga.—This rock is dark in colour, black to greyish black on fresh fractured surfaces. The texture of the ground mass is subophitic with lath-shaped felspars and interstitial augite. The texture of the rock as a whole can be described as holocrystalline porphyritic with phenocrysts of plagioclase. Labradorite and Enstatite augite are the essential constituents with apatite and iron ores as accessories. Brown plagonite glass is observed.

Basalt from Rutlam.—It is fine-grained (anamesite). The texture is glomeroporphyritic texture of Judd in which there is normal intersertal texture in the ground mass which contains groups of plagioclase crystals. Labradorite, augite, iron ores and glass are the constituents.

Eclogite (Glenelg district, Southerlands, Scotland).—These rocks illustrate the principle of minimum volume, the influence of which can be seen not only in the essential minerals, garnet and omphosite but also in the characteristic accessory mineral rutile. The retrograde change is amphibolisation. The amphibole is hornblende. The texture is granoblastic. Quartz is also present.

4. Results

Plates perpendicular to three mutually orthogonal directions, taking easy breakage plane as reference, are cut for each rock under investigation. Velocities of longitudinal ultrasonic waves with frequencies ranging from 1 to 12 megacycles along the thickness directions are determined. The differences of the extreme values of the velocities of each rock are expressed as percentages under the column "Anisotropy" after rounding off to the first significant figure. Effective elastic constants are calculated and they are represented in the tables along with densities. There are small variations in the densities in the same specimen for plates of different orientations. The variations can be attributed to the fact that the cross-sectional character of the units is not the same in all directions. The results on the sedimentary rocks are given in Table I while those on the igneous rocks are given in Table II.

5. Discussion of Results

(*a*) *Anisotropy*.—Results given in Tables I and II show that there is an intimate relationship between the propagation of elastic waves and the structural trends of the rocks. The amount of anisotropy depends on the state of stress enjoyed by the material.

Bhima limestone is a good example of a specimen subjected to load or static metamorphism. So the velocities in the two sections perpendicular to easy breakage directions are equal. Grey Hyderabad marble and Pink Rajaputana marble are impure calcareous sediments metamorphosed by stress and temperature. Consequently the velocities are not equal in the three directions. Jeffreys (1929) has suggested the possibility of sedimentary rocks being anisotropic due to the stratification of the layers.

In the case of igneous rocks, the velocities in the three directions are different. Anisotropy increases with the influence of stress. Eclogite shows the least difference which is almost negligible. This is in conformity with the nature of its genesis namely, that it is a plutonic rock formed essentially by hydrostatic pressure at great depths. That the velosity of propagation of sound waves is different in different directions suggests that deep in earth's crust where there are large differential stresses, it will be incorrect

TABLE I. *Sedimentary Rocks*

Name of Rock	Section parallel to easy breakage			Section perpendicular to easy breakage			Section perpendicular to both the directions			Anisotropy
	Density gm./cm.^{3}	Velocity km./sec.	Effective elastic constant dynes/cm.^{2}	Density gm./cm.^{3}	Velocity km./sec.	Effective elastic constant dynes/cm.^{2}	Density gm./cm.^{3}	Velocity km./sec.	Effective elastic constant dynes/cm.^{2}	
Bhima limestone ..	2·700	6·18	$10·33\times10^{11}$	2·721	5·10	$7·04\times10^{11}$	2·704	5·09	$7·07\times10^{11}$	18%
Kurnool limestone ..	2·697	6·72	12·19	2·647	4·17	4·61	2·682	3·97	4·21	41%
Jubbalpore marble ..	2·853	6·46	11·91	2·84	5·57	..	..	..	..	14%
Gray Hyderabad marble	2·071	5·68	6·69	1·582	4·80	3·64	1·575	4·71	3·50	17%
Rajaputana marble ..	2·71	6·41	11·13	2·704	4·33	5·08	2·689	4·28	4·91	33%

TABLE II. *Igneous Rocks*

Name of the Rock	Section parallel to easy breakage			Section perpendicular to easy breakage			Section perpendicular to both the directions			Anisotropy
	Density gm./cm.^{3}	Velocity km./sec.	Effective elastic constant dynes/cm.^{2}	Density gm./cm.^{3}	Velocity km./sec.	Effective elastic constant dynes/cm.^{2}	Density gm./cm.^{2}	Velocity km./sec.	Effective elastic constant dynes/cm.^{2}	
Kondavidu granite ..	2·620	6·57	$1·13\times10^{12}$	2·623	5·98	$0·94\times10^{12}$	2·614	4·74	$0·59\times10^{12}$	28%
Pink Hyderabad granite	2·607	6·62	1·14	2·604	6·54	1·11	2·618	4·80	0·60	28%
Gneiss ..	2·684	6·29	1·06	2·788	5·48	0·83	2·764	4·32	0·52	31%
Leptynite ..	..	..	..	2·659	5·48	0·80	2·687	4·46	0·53	18%
Keratophyre ..	2·642	6·21	1·02	2·581	6·10	0·96	2·571	4·92	0·62	21%
Chloritised dolerite ..	3·086	7·84	1·90	2·995	6·91	1·43	2·953	4·58	0·62	41%
Norite ..	3·080	6·85	1·44	3·069	6·34	1·23	3·042	5·90	1·059	14%
Dunite ..	3·262	8·27	2·23	3·211	7·55	1·83	..	..	..	8·8%
Deccan trap (Rutlam)	2·863	8·58	2·11	2·886	6·93	1·39	2·860	6·40	0·97	19%
Deccan trap (Gulberga)	2·767	8·61	2·05	2·777	6·97	1·35	..	..	..	25%
Eclogite ..	3·364	7·84	2·07	3·36	7·84	2·07	3·353	7·78	2·03	·7%

to represent the elastic behaviour of rocks as that of a single homogeneous isotropic solid.

As a result of extensive seismic surveys over an oil producing limestone in south-western Persia, two velocities were obtained by seismic methods. Richards (1933) explained this fact by saying that for a limestone there is no uniformity in elastic behaviour. It has, however, to be presumed that no further work was done in this direction as to a querry by Andrews in the discussion, he replied that "No evidence of the accuracy of anisotropy was sought as the experiments were mainly concerned with the velocities in directions parallel to the bedding plane and plates were cut to fulfil this condition."

Ide's results show that for dunite there is a change of velocity of 2% observed in two directions even at 4000 atmospheres. This change is attributed by Birch to porosity and he contends that at greater pressures the rocks behave isotropically. There is a marked variation of the velocity with the application of pressure. The magnitude of the observed change suggests change of substance not contemplated by the theory of elasticity. Porosity is inherent in every rock type and depends on the condition of formation of the rock. If this be subjected to prolonged pressures and temperatures of the magnitude used by the previous workers it will change its mineralogical composition though the chemical constitution may not change. Hence under such circumstances an entirely new rock may result. Thus in these experiments though basaltic rock behaves anisotropically, eclogite which has the same basaltic composition but different mineral assemblage due to the influence of static pressure shows the least anisotropy. In view of these observations, the theory that rocks behave in the same way even at low pressures as they do under 12000 atmospheres is no longer tenable.

From a scrutiny of the published data with regard to the velocity of propagation of sound in rocks, a great variation is apparent. For example the reported longitudinal velocity in granites varies from 5 km.sec. to 6·24 km.sec. One of the factors contributing to this variation is that the velocities calculated from the compressibility data are incomplete. This does not, however, explain completely the reported variation. It has to be recognised that the elastic properties show variation in rocks depending upon the directional disposition of the specimen selected. It is interesting to note that this range of variation is within the extreme values found for granites in the present investigation—4·32 km.sec. to 6·62 km.sec. depending on the direction of selection of the specimen. Similarly the variation for other rocks also can be attributed to the selection of the specimen in different directions.

(*b*) *Interpretation of seismic results.*—In the interpretation of seismic results many discrepancies are met with. Jeffreys (1929) suggest that the earth's crust may be regarded as made up of thin layers of different mechanical properties with the hope that they may offer an explanation of the seismic observation.

In a recent paper Gutenberg (1945) attempted to study the variation of the velocity of longitudinal seismic waves with the depth. He assumed that the velocity at a depth '*h*' is given by

$$V_h = V_o + bh,$$

where *b* is a constant varying from layer to layer. This assumption however, does not explain the low velocities in the uppermost layers of 1 to 2 kilometers. Gutenberg suggests that "Improvements would consist in a more accurate determination of the factor *b* and in assuming a better functional relationship between V and *h*." The results of the present investigation indicate that the clue lies in the second alternative. It can be seen that directional relationships would manifest themselves very strongly in the uppermost layers, thus accounting for the low velocities.

(*c*) *Validity of postulation of new layers.*—Several Geophysicists have postulated different crustal layers from the study of the velocity of propagation of seismic waves. In view of the proved anisotropic behaviour of rocks, the mere differences in the velocities of propagation of seismic waves cannot be regarded as a sufficient criterion for postulating different crustal layers.

6. Summary and Conclusion

The advantages of the wedge method developed by Bhagavantam and Bhimasenachar for the determination of elastic properties of rock sections are discussed. The experimental technique underlying the above method is briefly described. From a systematic investigation of different rock sections, it is shown that there is a definite anisotropy with regard to their elastic behaviour. In the case of sedimentary rocks, the velocity is higher in a direction perpendicular to the bedding or cleavage plane. The value of the velocity is greatest in a direction normal to the rift plane in the case of granites and to the easy breakage direction, in other igneous rocks. It is least in a direction normal to the hard way plane of granites.

The amount of anisotropy appears to be a function of the stress experienced by the rock. The special behaviour of eclogite, in that the velocity is almost the same in all the directions, is in conformity with the nature of its genesis, namely, that it is a plutonic rock formed essentially by the hydrostatic pressure at great depths.

It is pointed out that correct inferences cannot be drawn regarding the nature of the crustal layers from divergent results obtained through seismic data alone. The anisotropic nature of the rock through which the waves are propagated has also to be taken into account. The importance of the realisation of this fact in the interpretation of seismic data is indicated.

In conclusion, I have pleasure in acknowledging my thanks to Professor C. Mahadevan and Professor S. Bhagavantam for suggesting the problem and for their direction of the research. To Dr. J. Bhimasenachar I am deeply indebted for his constant help and advice.

References

1. Adams and Coker .. *Carnegie Inst. Wash. Pub.*, 1906, No. 46, 69.
2. —— and Gibson .. *Gerl. Beitr.*, 1931, **Bd. 15**, 241–50.
3. —— and Gibson .. Papers from *Geophy. Lab. Carnegie Inst. Wash.*, 1931, No. 770.
4. —— and Williamson .. *Jour. Franklin Inst.*, 1923, **195**, 475–579.
5. Bhagavantam and Bhimasenachar .. *Proc. Ind. Acad. Sci.*, 1944, **20**, 298.
6. Birch, Bancroft & Dennison *Jour. Geol.*, 1938, **46**, 59–87, 113–41.
7. —— and Dow .. *Bull. Geol. Soc. America*, 1936, **47**, 1235.
8. Birch .. *Jour. Applied Physics*, 1937, **8**, 129.
9. ———— .. *Jour. Geol.* 1940, **148**, 752–66.
10. ———— .. *Bull. Geol., Soc. America*, 1943, **54**, 63–86.
11. Bridgman .. *Proc. Amer. Jour. Sci.*, 5th series, 1924, **7**, 81–102.
12. ———— .. *Amer. Jour. Sci.*, 5th ser., 1925, **58**, 483–98.
13. Bruggeman .. *Elastizitat Konstanten von Kristallaggregaten*, The Hague, 1930.
14. ———— .. *Ann. Der. Phys.*, 1937, **29**, 160.
15. Grimme .. *Phil. Mag.*, 1935, **20**, 304.
16. Gutenberg .. *Amer. Jour. Sci.*, 1945, **243 A**, 285–312.
17. Ide .. *Proc. Nat. Acad. Sci.*, 1933, **22**, 81–91, 482–96.
18. ———— .. *Jour. Geol.*, 1937, **45**, 689–716.
19. ———— .. *Rev. Sci. Inst.*, 1935, **6**, 295–98.
20. Jeffreys .. *The Earth, Its Origin, History and Its Physical Constitution*, 1929, 2nd ed., Cambridge, pp. 85–100.
21. Karman .. *Zeit. D. Ver deutschen Ingenieure*, 1911, **55**, 1749–57.
22. Kausakabe .. *Jour. Coll. Sci. Tokyo.*, 1904–05, **20**, Art. 10.
23. Richards .. *Proc. Phy. Soc. London*, 1933, **45**, 70–81.
24. Roess .. *Comptes Rendus*, 1935, **200**, 147–49.
25. Zisman .. *Proc. Nat. Acad. Sci.*, 1933, **19**, 653.

INTERACTION OF NITROUS OXIDE, NITROGEN AND PHOSPHORUS UNDER SILENT ELECTRIC DISCHARGE

By G. S. Deshmukh, M.Sc., and Y. D. Kane, M.Sc.
(Asstt. Prof. of Chemistry, Benares Hindu University)

Received November 26, 1946
(Communicated by Prof. S. S. Joshi, D.Sc., F.A.Sc.)

The thermochemical behaviour of a number of gases towards phosphorus, particularly its glow, has been studied by various workers.[1] There is, however, but little quantitative information in the literature on the production of these changes under well-defined conditions of electrical discharge. Joshi[2, 3, 4] gave an important lead in this field of research in observing the general utility of data for the time-variation of the discharge current, in the elucidation of the mechanism of the corresponding reaction. This is illustrated by numerous results in these laboratories, especially on the reduction with hydrogen of gaseous nitrous oxide and in frozen films at liquid air temperature.[5, 6] It was of interest therefore, to extend these observations to a study of the reaction between the phosphorus films and nitrous oxide, under silent discharge.

Experimental

The general arrangement of the apparatus and circuit employed are shown in Fig. 1. A Siemens' type ozoniser made with soft glass tubes (fitted co-axially with a rubber greased ground-joint) was surrounded by a tube filled with salt solution, to serve as a low tension electrode. The whole system was immersed in a jacket, in which a stream of water was kept flowing at a constant rate in order to minimise the heat effects under the discharge. The ozoniser was connected through tap 1 to a mercury manometer and through tap 2 to a Töpler. Nitrous oxide obtained from a commercial cylinder was admitted through tap 8 and stored in glass reservoirs R_1 and R_2 which had been evacuated previously. With taps 8, 10 and 5 closed, on opening tap 7, most of the nitrous oxide was frozen to a solid of negligible vapour pressure in traps cooled by liquid air in Dewar vessels D_3 and D_4. The uncondensible gases were removed through tap 5 by the Töpler, tap 2 being closed. Dewar vessels D_3 and D_4 were then carefully removed; the first portion of the frozen gas to vaporise was pumped out; tap 5 closed; and the middle fraction stored in R_1 and R_2 after toplering off through tap 5 the last part of the condensed gas to vaporise. After the entire assembly

of the apparatus was tested for vacuum for at least 48 hours, taps 3 and 1 were closed. The inner electrode of the ozoniser was then coated uniformly on the outside with a concentrated solution of phosphorus in carbon disulphide, and fitted in the ozoniser system. The solvent was removed first with a hyvac pump from tap 3 and finally on the Töpler. At the commencement of every experiment nitrous oxide from R_1 and R_2 was frozen in traps cooled by liquid air in D_3 and D_4; the middle fraction of the vaporised gas was led over a train of tubes charged with P_2O_5 and KOH, and introduced into the annular space of the ozoniser through tap 3 at the desired pressure.

The A.C. obtained by means of a 1 K.W. Rotary Converter worked off 220 volt, D.C. mains was fed to the primary of a 3 KVA transformer; one of its secondaries was earthed; the other connected serially through a 10,000 ohm stabilising resistance, was dipped in the salt solution forming the inner electrode of the ozoniser. The outer electrode was earthed through an oxide rectifier type A.C. micro-ammeter μA (see Fig. 1). The applied

INTERACTION OF PHOSPHORUS WITH N_2 AND N_2O UNDER ELECTRIC DISCHARGE.

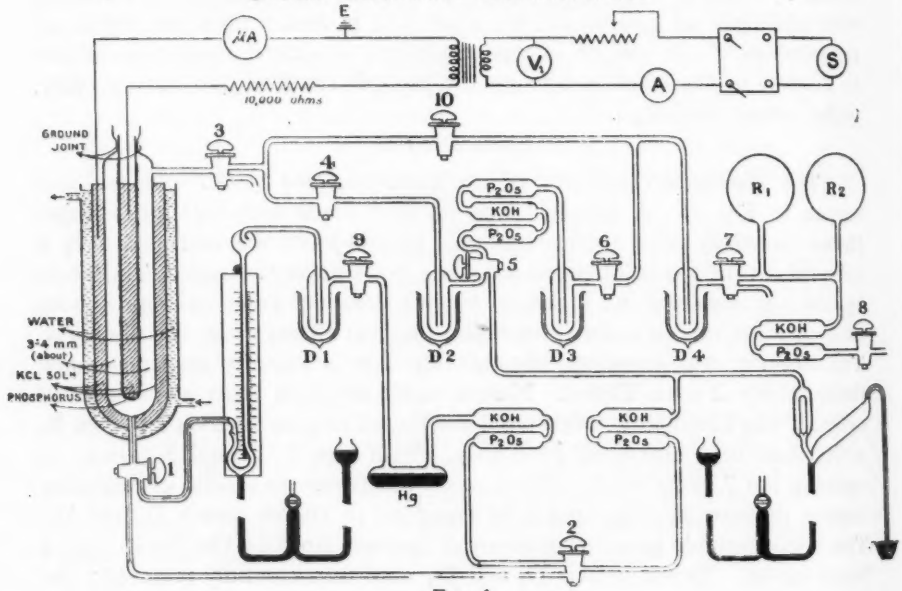

FIG. 1

potential expressed in kilo-volts (r.m.s.) and called V, was calculated from a knowledge of the stepping up ratio of the transformer and of the primary

potential, V_1; the latter was regulated by means of a variable resistance in its primary.

Discussion of Results

Series of experiments started at various gas pressures were made on the nitrous oxide-phosphorus reaction under conditions mentioned above; a fresh film of phosphorus was employed in each series. In agreement with a general finding due to Joshi,[2, 3, 4] on changes under electrical discharges especially in gases, the interaction between nitrous oxide and phosphorus sets in only above a characteristic 'threshold potential' V_m, where the material in the annular space breaks down as a dielectric. V_m depends, *inter alia*, on the gas pressure p and frequency of the electrical supply. The course of the reaction was followed by observations at regular intervals of the gas pressure p at constant volume, and also of the corresponding discharge current i. These data for one typical series corresponding to a nitrous oxide pressure of 12·2 cm. Hg, and 4 kilo-volts (r.m.s.) for the secondary potential of 50 cycles frequency are shown in Fig. 2. In all cases observed, p decreased progressively during, and was negligibly small at the end of, the reaction. A further continuation of the discharge even at enhanced V the secondary potential had no effect as judged from the constancy of the spectral nature of the glow and of the gas pressure p. As shown by the total time for the reaction and especially by the average time-rate of the pressure decrease, the rate of the change increased with V and 1/p. This follows readily from Joshi's general finding that the 'threshold potential' V_m increases with p and that the rate of a discharge reaction and the corresponding i depend (increase with) on $V\text{-}V_m$.[2, 3, 4]

As observed by Joshi[2, 3, 4] in the decomposition of (pure) nitrous oxide under silent discharge, the current i varied sensibly discontinuously during the present reaction at a given V, indicative of consecutive changes (see Fig. 2). Thus, for example, during the short initial stage when p diminished, i increased appreciably. In the next stage which was the longest, both these quantities varied comparatively slowly. The last stage is characterised by a remarkably sudden and rapid decrease of i to a constant minimum at which p also becomes negligibly small, suggestive of the completion of the reaction. From results of a number of reactions at various initial p and V, of which the curves in Fig. 2 are one typical illustration, it was found that the last stage during which i dropped suddenly, commenced when the residual p of the reaction mixture reached 3 to 6 mm., *i.e.*, about 4 per cent. of the initial p. This sudden drop of i at a constant V, was also observed when nitrogen was used instead of nitrous oxide (Fig. 3).

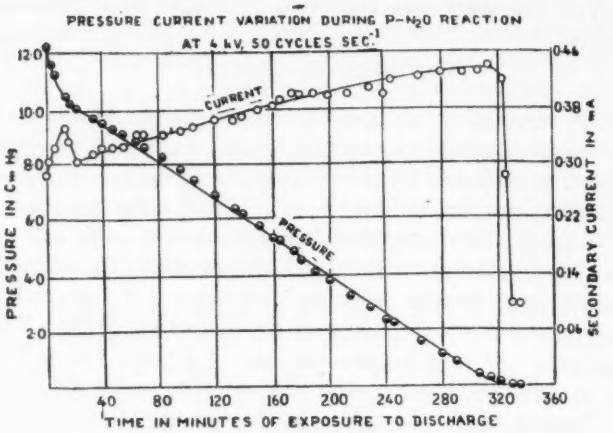
PRESSURE CURRENT VARIATION DURING P-N2O REACTION
AT 4 kV, 50 CYCLES SEC.-1
CURRENT
PRESSURE
PRESSURE IN C-m Hg
SECONDARY CURRENT IN mA
TIME IN MINUTES OF EXPOSURE TO DISCHARGE

FIG. 2

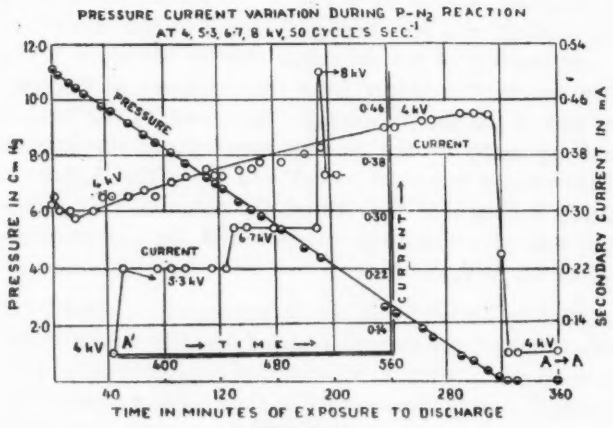

FIG. 3

The observed decrease in the over-all p (as also the corresponding changes) are explicable, on the following mechanism for the reaction:

$N_2O \rightarrow N_2 + O$ (*ia*) (The *atomic products* in (*ia*), (*ib*) and (ii) are
$N_2O \rightarrow NO + N$ (*ib*) removed immediately by phosphorus).
$NO \rightarrow N + O$ (ii)

Changes (*ia*) and (*ib*) occur simultaneously and represent the initial stages; (*ia*) is suggested to be the more predominant reaction. This agrees with Joshi's results for the decomposition of (pure) nitrous oxide under

silient discharge;[2,4] mixed with an excess of hydrogen;[5] and when frozen over glass and certain metallic receptacles at the liquid air temperature.[6] Atomic oxygen and nitrogen produced in (*ia*) and (*ib*), react with the phosphorus film, the former practically instantaneously. The fact that free oxygen was not detected in the reaction mixture at any stage is in accord with this deduction. So far as the gas phase is concerned, the net change represented by this stage (*ia* and *ib*) is $2N_2O \rightarrow NO + N_2$ since the other (atomic) products, *viz.*, N and O being removed by phosphorus do not contribute to the gas pressure. It follows from this, that the gas pressure during this stage of the reaction should be constant. This anticipation was realised experimentally by working on the following suggestion due to Prof. Joshi:[3] It is to reduce the over-all velocity to a minimum by maintaining just V_m on the ozoniser, so that the otherwise rapid and even transient reactions are slowed sufficiently to enable observations of their time-rate and also the nature of the corresponding products, which ordinarily would escape detection. With this restraint a definite though short lived stage during which *p* remained sensibly constant was observed initially in a number of N_2O — P reactions under the discharge. It may be emphasized here that the discontinuous time-variation of *i* characteristic of the stage-wise progress of this reaction (Figs. 2 and 3) was more conspicuous when V did not exceed V_m appreciably as is to be expected from Joshi's views.[3] Studies of other types of discharge reactions in progress in these laboratories have shown the wide applicability of this device, *viz.*, excitation at V_m for elucidating the characteristic course and mechanism of a discharge reaction.[3]

Since according to Joshi,[2,3,4] $V\text{-}V_m$ determines *i*, its rise in the initial stage (see Fig. 2) may be attributed to a reduction of the corresponding V_m, due firstly, to N_2O changing to NO and nitrogen; and secondly, due to phosphorus being replaced by its oxide (and possibly nitride, *vide infra*). This deduction agrees with the observation by various workers that the oxidation of phosphorus produces ionisation in the surrounding air;[7] and also with our experimental results with phosphorus films reacting with air (dried carefully with the arrangement shown in Fig. 1) subjected to the ozoniser discharge at 27·2, 31·4, 47·9, 53·4, 60·0, 65·7 and 73·2 cm. Hg pressures at V varied from 1 to 5 kV of 50 cycles frequency, and the time of exposure to discharge being increased up to 3·5 hours. It was always found that *whilst p decreased, the corresponding i increased markedly.*

The decomposition of nitric oxide according to (ii) constitutes chiefly the next stage. Its atomic products would be removed from the gas phase, oxygen especially being affected very much faster due to its much

greater affinity towards phosphorus. The production of nitric oxide was detected in a series of experiments at various initial pressures on nitrous oxide (a fresh film of phosphorus being used in every case) by introducing from tap 3, a small bubble of air in the ozoniser after exposure to discharge for about 3–5 minutes; this reaction mixture when led over a small amount of pure mercury (shown by Hg, in Fig. 1) fouled it immediately due to formation of nitrogen dioxide; this was never observed after longer exposures; and also *in absence of air* when the mixture was toplered out at any stage of the reaction. Nitric oxide occurs therefore, in the present reaction as an intermediate product during only early stages. This conclusion was confirmed further by analysis of mixtures from reactions at various initial pressures of nitrous oxide in the range 15 to 42 cm. Hg; the discharge was interrupted after different periods of exposure. The mixture was led by opening tap 1 and lowering the manometric mercury in M, through a trap cooled by liquid air in D_1 in order to separate nitrous oxide; nitric oxide also freezes to a solid with a small sublimation pressure and can therefore, be toplered out completely from tap 2. The mixture thus pumped out consisting of nitric oxide and nitrogen was collected in a gas burette and analysed for nitric oxide by absorption with acidified ferrous sulphate solution. In no case was nitric oxide observed after 10 minutes *i.e.*, after about 1/30th of the total time for the reaction; furthermore, the ratio NO/N_2 in the mixture increased as the time of exposure was reduced. Nitrous oxide does not react with phosphorous thermochemically " even when touched with a piece of red hot iron."[8] At higher temperatures it inflames, " the products being phosphorus pentoxide and pure nitrogen dioxide."[8] This last is also observed when nitric oxide is substituted for nitrous oxide in the thermal change. It is not unlikely that nitric oxide is formed as an intermediate product at very early stages of the high temperature reaction between phosphorus and nitrous oxide by analogy with the present results for the discharge reaction. The latter differs from the purely thermal change, in that nitrogen dioxide is not observed at any stage. Presumably, this applies also to the interaction under discharge, with nitric oxide (*vide infra*).

A series of experiments was next carried out in order to investigate the removal by phosphorus of nitrogen from the gas phase, produced by the decomposition of N_2O and NO according to (*ib*) and (ii). The ozoniser in Fig. 1 was filled with cylinder nitrogen (after bubbling slowly through traps containing freshly prepared alkaline pyrogallol in order to remove traces of oxygen) at 7·0, 8·0, 9·0, 11·3, 12·7 and 21·5 cm. pressures and subjected to discharge at V varied in range 2–4 kV at 50 cycles frequency for periods up to 12 hours. In every case p diminished and the correspondin g

i increased. Towards the end of the reaction, i dropped remarkably suddenly; curves in Fig. 3 refer to a typical run with 11·3 cm. of nitrogen at 4 kV. The general resemblance of the progress of this reaction, as shown by the time-variation of i and p with that, when nitrous oxide (initial p and applied V being smaller) was used instead, is also striking. For the nitrous oxide-phosphorus and nitrogen-phosphorus reactions at the same potential *viz.*, 4 kV and similar initial pressures 12·2 cm. N_2O and 11·3 cm. N_2 (see Figs. 2 and 3), the total time for the reaction, *i.e.*, when the gas pressure became negligibly small, was 340 and 330 minutes respectively; this similarity is suggestive. As with nitrous oxide, after its final sudden drop to a minimum, on increasing V, i first increased (almost) momentarily to a large value; this remained stationary as long as the corresponding V was constant (see Fig. 3).

If after the removal of nitrogen by phosphorus, a further amount of it was introduced, p and $1/i$ continued to decrease, but on the whole more slowly than before. Thus *e.g.*, in one experiment at 4 kV and initial p of 11·4 cm. Hg of nitrogen, 50 per cent. of the pressure change occurred in 160 minutes; the total time required was about 330 minutes. At the end of this period, when p became negligibly small (see Fig. 3) fresh nitrogen was introduced at 4 cm. pressure in the ozoniser. It now took about 290 minutes for the same, *i.e.*, 50 per cent. pressure change, despite a larger reaction rate due to $1/p$ and V (6 kV) being greater than before. With 21·5 cm. pressure due to a further addition of nitrogen, exposures to discharge at 10·7 kV for 39 hours produced only 60 per cent. of the total pressure decrease. Detailed experiments showed that any thermo-chemical change between the phosphorus film and the nitrogen (also air) in the ozoniser was negligibly small compared with that produced under the discharge. It was also noticed incidentally during this stage, that the 'threshold potential' V_m characteristic of the aerial oxidation of phosphorus by an ozoniser discharge is defined more sharply, if the inner electrode supporting the phosphorus film is cooled (to about 3° C.) than at the room temperature *viz.*, 27° C. It was also found that changes in the appearances of the glow from initial violet to yellow; and of the electrode film of phosphorus from white to yellow, brown and finally almost black, were comparatively more distinct.

Results for the nitrogen-phosphorus reaction under discharge due to fields at 500 cycles and also much higher frequencies obtained with a serial spark, were found to be on the whole similar to those observed at 50 cycles frequency (Fig. 3).

Examination under microscope of the products (of a number of reactions) on the inner electrode after long exposures to the discharge showed

small crystals of (unused) yellow phosphorus mixed with a brown substance. The mixture on treatment with water gave ammonia when treated with Nessler's reagent, indicating that a phosphorus nitride was produced under the discharge. Using Geissler type discharges and metallic electrodes, Strutt[9] (now Lord Rayleigh) found that phosphorus absorbed nitrogen, and that the gas was not reliberated on heating, which he attributed to the formation of a chemical compound; this agrees with the results of Newman,[9] and Moldenhauer and Dörsom.[10] In the present work (*vide supra*), the reaction products always revealed a nitride; its formation would appear therefore, to represent by far the main change in the $P-N_2$ interaction under the silent discharge. Judged by the time-rate of the variation of both p and corresponding i, this 'clean up' of nitrogen by phosphorus was more rapid as the applied V and 1/p were increased; ultimately, whole of the input nitrogen was removed. As observed in the last stage of each of the reactions with nitrous oxide also (see Fig. 2), when the pressure of the residual nitrogen was very small, i decreased remarkably suddenly. This supports the deduction made that the decomposition under discharge of nitric oxide is completed during early stages; and that the 'clean up' of nitrogen is practically the only change, which constitutes a later and by far the longest stage in the N_2O-P interaction under discharge. The remarkably sudden drop of the current i (*cf.* Figs. 2 and 3) to stationary values at the end of $P-N_2O$ and $P-N_2$ reactions may be attributed to the production of a vacuum condition in the discharge space by the final 'clean up' of nitrogen by the phosphorus film, which is practically the same sole change during the latter part of both the above reactions; incidentally, this illustrates the marked 'getter' action of phosphorus. The current i is constant as long as V is constant *e.g.*, at 4 kV in Fig. 3; it, however, increases immediately to a higher constant value (*cf.* the step-wise, current-time curve, continued from A to A′ in Fig. 3) owing to increased ionisation of the residual gas (and phosphorus vapour) under fields due to larger V.

On general considerations, it is shown easily that the discharge current i in a gas under a constant applied field would increase as p is reduced, since the energy gained by motion under the field by an ion (chiefly electron) at the end of a given free path increases with its length *i.e.*, with 1/p; the limitation, due to the circumstance that the total number of electrons leading to ionisation and therefore, contributing to i also diminishes with p, is not large. At moderate pressures, obtained during the main course of the reaction of N_2O and nitrogen with phosphorus, i is maintained as a balance of two factors mentioned above; on the whole, i tends to increase as the pressure is diminished (see Figs. 2 and 3), except when it becomes negligible

towards the end of both these reactions. The large though momentary rise of i on applying 8 kV before the attainment of the final stage (Fig. 3) in this nitrogen-phosphorus interaction requires, however, further investigation.

In conclusion, we welcome this opportunity of expressing our sincere and grateful thanks to Professor S. S. Joshi, D.Sc. (London), F.A.Sc., Head of the Chemistry Department, for suggesting the problem, instructive advice and kind encouragement during this work.

Summary

Interaction with phosphorus films of nitrous oxide, nitrogen and oxygen in silent discharge under fields due to potentials (V) of 50, 500 cycles and the high frequencies has been studied at various pressures p. In agreement with a general finding due to Prof. Joshi,[2, 3, 4] the change sets in above a minimum V_m and that both the current i and the reaction rate at a given V depend upon $V-V_m$. p decreases progressively to zero, when the reaction terminates; this is characterised by a remarkably sudden drop of the corresponding i. Free O_2 is not observed; NO occurs only at early stages. Two simultaneous changes (*ia*) and (*ib*), the former being the more rapid, followed by (ii) represent the reaction mechanism *viz.*, $N_2O \rightarrow N_2 + O$ (*ia*) $N_2O \rightarrow N + NO$ (*ib*) $NO \rightarrow N + O$ (ii). The atomic products react with phosphorus immediately. Removal of molecular N_2, from (*ia*) and that formed by recombination of N from (*ib*) and (ii) by phosphorus, is the longest stage. Phosphorus nitride is the chief product with both N_2O and N_2. The time-variation of i is markedly synchronous with, but more pronounced than that of p; and more helpful in revealing the stages of the reaction, suggested as a general proposition by Joshi.[3] Interaction with oxygen produces a rise of i in striking contrast with that with nitrogen.

References

1. *Cf.* Melville and Ludlam .. *Proc. Roy. Soc.*, 1931, A **132**, 108–26.
2. Joshi .. *Trans. Faraday Soc.*, 1929, **25**, 118–2 ; 137–43.
3. ———— .. *Curr. Sci.*, 1946, **15**, 281; 1939, **8**, 518.
4. ———— .. *Trans. Faraday Soc.*, 1927, **23**, 227.
5. ——— and Deshmukh .. *Nature*, 1945, **155**, 483.
6. ———— .. *Proc. Indian Sci. Cong., Chem. Sec.*, 1939, Abst. 57; *ibid.*, 1940, Abst. 184.
7. *Cf.* Richardson .. "Emission of Electricity from hot bodies," Longmans, 1921, **6**, 302–3.
8. *Cf.* Mellor .. "Comprehensive Treatise of Theoretical and Inorganic Chemistry," Longmans, 1928, **8**, 787.
9. Strutt, *Cf.* Newman .. *Proc. Phys. Soc.*, 1921, **33**, 73–82.
10. Moldenhauer and Dörsom .. *Ber.*, 1926, **B 59**, 926.

THE SCATTERING OF LIGHT IN QUARTZ

By V. Chandrasekharan

(From the Department of Physics, Indian Institute of Science, Bangalore)

Received February 1, 1947

(Communicated by Sir C. V. Raman, Kt., F.R.S., N.L.)

1. Introduction

As is well known, when a beam of plane polarised light traverses a crystal of quartz along the optic axis, the plane of polarization is rotated continuously. The rotation increases very rapidly as the wavelength of the light diminishes: it is 26°, 42° and 148° per millimetre respectively for the wavelengths λ 5461, λ 4358 and λ 2537. If the crystal is viewed by an observer in a direction transverse to the beam, the electric vector in the light beam would be alternately parallel and perpendicular to the line of sight for each successive rotation of 90°. Hence, if the light diffused by the crystal is partially or completely polarised, the track of the beam as seen by the observer should exhibit alternate minima and maxima of intensity, the distance from one dark band to the next being the distance of travel of the incident beam in which there is a rotation of 180°. The widths of the bands for the wavelengths λ 5461, λ 4358, and λ 2537 would be 7·06, 4·33 and 1·22 millimetres respectively. A phenomenon of this kind was observed and photographed in *smoky quartz* with *visible light* by the present Lord Rayleigh (1919); it had its origin in the Tyndall scattering by the inclusions present in the crystal to which the smoky colour is ascribed. The present paper records the observation of the phenomenon in *perfectly colourless quartz* having its origin in the diffusion of light by the atomic vibrations in the crystal lattice. Both visible light λ 4358 and the ultraviolet radiation λ 2537 of the mercury arc in quartz have been successfully used to photograph the effect. Owing to the very great intensity of the resonance radiation emited by the water-cooled, magnet-controlled mercury arc which was employed, as also the large scattering power arising from the λ^{-4} law and the high rotatory power of quartz in the ultraviolet, the phenomenon is much more striking as observed with λ 2537 than with λ 4358 radiation.

2. Experimental Technique

For the purpose of the experiment, a perfectly colourless and transparent sphere of quartz crystal 5·24 centimetres in diameter was employed.

As was shown long ago by Sir C. V. Raman (1922), such a sphere in which no visible inclusions are present exhibits a uniform blue track when traversed by a condensed beam of sunlight. The use of a sphere is convenient as light can be sent in any required direction. To reduce the surface reflections, the sphere can be immersed in clean distilled water. When the beam of condensed sunlight traverses the sphere along its optic axis and the blue track is viewed transversely, the scattered light shows very marked polarization in which the electric vector is perpendicular to the optic axis. Again, when unpolarised sunlight is sent perpendicularly to the optic axis and the track is observed in a direction transverse both to the optic axis and to the beam of light, the scattered light is strongly polarised with most of the light having its electric vector parallel to the optic axis. However, when the observation is made along the optic axis with the light beam perpendicular to it, the scattered light is completely unpolarised. This is evidently due to the fact that scattered light before reaching the observer traverses the crystal along its optic axis and hence its plane of polarisation is rotated. The amount of rotation varies for the different wavelengths of sunlight and the emerging light hence appears to be completely unpolarised.

The foregoing observations indicated that the phenomenon of the bands could be expected and that for photographing them monochromatic light would have to be used. Another important condition for the successful performance of the experiment is that light should traverse the crystal along its optic axis pretty accurately. To secure this, the sphere is placed between two polaroids, and observed in mercury arc light and adjusted until the melatrope is observed centrally in the field of view with rings around it. By rotating the analysing polaroid clockwise, the rings of any particular colour appear to expand and hence the sphere rotates the plane of polarisation anticlockwise as viewed by the observer. The sphere is hence a left-handed crystal.

To photograph the phenomenon of the bands, the radiation of a water-cooled, magnet-controlled mercury arc was employed as the source of light and an aperture of 5/8" in diameter placed just in front of the arc limited the beam of light used. Actually, the whole radiation of the mercury arc was used, as the other wave-lengths were weak compared to the λ 2537 radiation and were also scattered comparatively feebly. The light beam was condensed by means of a 17 cm. lens of 4 cm. aperture into a brass cell fitted on opposite sides with two strain-free vitreous silica windows of 3 cm. aperture. The inside of the brass cell was painted black, and the quartz sphere

was placed inside it on an ebonite ring and was immersed in clean distilled water. The light before entering the brass cell was polarised by a large nicol which transmits the λ 2537 radiation. The sphere was adjusted so that the light traverses it along its diameter exactly parallel to the optic axis and there was thus no refraction of light at the surface of the sphere. The light emerging vertically from the surface of water was photographed by a camera fitted with a 6·5 cm. quartz lens of aperture 3 cm. and in this way a large quartz window for the observation was dispensed with. The camera and the top of the brass cell were wrapped up in a black cloth to prevent stray light entering the camera directly. A process plate was used and an exposure of one hour was given. A photograph of the track in the transparent quartz sphere showing a large number of bands was obtained, an enlarged reproduction of which is given at the end of the paper. Another photograph with a different arrangement, using the visible 4358 Å line of the mercury arc was also obtained, but a long exposure of 100 hours was needed for this purpose. Even so, the photograph was not dense enough to be satisfactorily reproduced.

3. Remarks

The width of the bands was measured and the magnification produced by the combination of the sphere, water and the camera was calculated. From this the actual width of each band was deduced. This distance should correspond to a rotation of 180° for the particular wave-length used, and hence enable the rotation per millimetre to be calculated for the two wavelengths λ 2537 and λ 4358 respectively. The results are given in the table below along with the standard values for comparison.

Table I

Wavelength in Å	Measured average width of each band in mm.*	Magnification of the system	Actual width of each band in mm.	Calculated rotation per mm. in degrees	Rotation per mm. in degrees from I. C. T.
2537	1·421 (22)	1·340	1·085	165·9	148·6
4358	4·133 (3)	0·97	4·25	42·4	41·6

* The number in the brackets gives the total number of bands measured whose average width is given.

The fair agreement between the calculated and the actual rotations and the uniform clarity of the bands indicates the highly monochromatic nature of the light scattered and that the other radiations are not recorded. The contrast between the maxima and minima of intensity of the bands

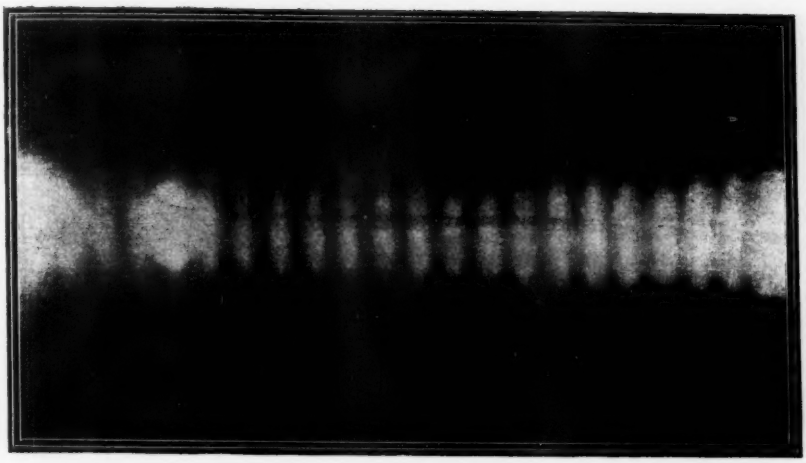

FIG. 1

Track of polarised λ 2537 beam traversing quartz along optic axis

shows that the scattering of light in quartz is well polarised. The picture of the bands reveals at a glance the continuous rotation of the plane of polarisation taking place inside quartz and the marked polarisation of transversely diffused light in quartz arising from the atomic vibrations in the crystal lattice.

As will be noticed, the bands are not straight, but are slightly curved. This is because the surface at which light enters the quartz crystal is curved, and hence the points of equal rotation lie along a curve parallel to the surface.

In conclusion I wish to thank Sir C. V. Raman for suggesting the problem and for his constant encouragement. I wish also to take this opportunity to express my grateful thanks to Dr. R. S. Krishnan for his kind help which was always available.

Summary

When a plane-polarised beam of the intense λ 2537 radiation from a water-cooled, magnet-controlled mercury arc is sent along the optic axis of a perfectly clear and transparent sphere of quartz crystal free from inclusions, the track when photographed from a direction transverse to the beam exhibits striking fluctuations in intensity along its length. The effect, which is reproduced in the paper, is obviously connected with the rotation of the plane of polarisation of the polarised λ 2537 radiation as it traverses the crystal. The distance between one dark band to the next corresponds closely to a rotation of 180° of the plane of polarisation of the λ 2537 radiation. A similar effect was observed and photographed in smoky quartz by the present Lord Rayleigh in 1919 using the Tyndall scattering of visible light by the inclusions in the crystal. In the present case the effect is due to the diffusion of light arising from the atomic vibrations in the crystal lattice, and the clearness of the bands indicates that such scattering is strongly polarised.

References

1. Strutt, R. J. .. *Proc. Roy. Soc.*, 1919, **95**, 476.
2. Raman, C. V. .. *Nature*, 1922, **109**, 42.
3. ———— .. *Molecular Diffraction of Light*, 1922, p. 76.

THE DISPERSION, BIREFRINGENCE AND OPTICAL ACTIVITY OF QUARTZ

By T. Radhakrishnan

(From the Department of Physics, Indian Institute of Science, Bangalore)

Received January 27, 1947

(Communicated by Sir C. V. Raman, Kt., F.R.S., N.L.)

1. Introduction

As is well known, quartz is a uniaxial crystal exhibiting optical activity and its behaviour in respect of radiations of specified wave-length to which it is completely transparent may be specified by three constants, *viz.*, its ordinary refractive index n_ω, extraordinary refractive index n_ϵ, and rotatory power ρ (along the optic axis), in degrees per millimetre. The accurate measurement of these quantities has been the subject of many investigations and various attempts have been made to express the experimental data and their dependence on the radiation frequency by appropriate formulæ. The experimental work and the formulæ proposed up to 1927 are reviewed in Sosman's *The Properties of Silica* (1927) and Lowry's *Optical Activity* (1935).

Besides the literature reviewed in these treatises some contributions to the subject may also be mentioned here. New formulæ have been proposed by Coode-Adams (1928), Bradshaw and Livens (1929) and Engl (1936). There has also appeared a detailed analysis of the infra-red absorption of quartz by Saxena (1940). Servant has extended the measurements on optical activity to 1525 Å.U. (1938) and determined the birefringence up to 1450 Å.U. (1937). The spectroscopic behaviour of quartz has been investigated in detail by Tousey (1940) in the remote ultra-violet.

The formulæ so far proposed give values which steadily deviate from the newer measurements with diminishing wave-length. This is perhaps not surprising since the absorption frequencies in the older formulæ (especially in the ultra-violet) are empirically assumed ones. Accordingly, in the present investigation, the author has tried to derive new formulæ which are free of these defects.

2. The Formulæ Proposed

These are

$$(1)\quad n_\omega^2 = 4{\cdot}57877 + \frac{0{\cdot}003952}{\lambda^2 - 0{\cdot}014161} + \frac{0{\cdot}003808}{\lambda^2 - 0{\cdot}011236} + \frac{0{\cdot}003114}{\lambda^2 - 0{\cdot}000974} + \frac{44{\cdot}224}{\lambda^2 - 78{\cdot}22} + \frac{713{\cdot}55}{\lambda^2 - 430{\cdot}55}$$

$$(2)\quad n_\epsilon^2 = 4{\cdot}730561 + \frac{0{\cdot}0042647}{\lambda^2 - 0{\cdot}014161} + \frac{0{\cdot}0041290}{\lambda^2 - 0{\cdot}011236} + \frac{0{\cdot}0028067}{\lambda^2 - 0{\cdot}000974} + \frac{41{\cdot}678}{\lambda^2 - 77{\cdot}3} + \frac{701{\cdot}354}{\lambda^2 - 388}$$

$$(3)\quad \rho = \frac{4{\cdot}948}{\lambda^2 - 0{\cdot}014161} + \frac{4{\cdot}617}{\lambda^2 - 0{\cdot}011236} - \frac{2{\cdot}311}{\lambda^2 - 0{\cdot}000974} - \frac{0{\cdot}000815}{(\lambda^2 - 0{\cdot}0195)^2} - 0{\cdot}1905$$

(λ, in all cases, is in microns.)

These formulæ are largely refinements on the work of Coode-Adams and Lowry. The first two ultra-violet terms, with peaks at 1190 Å.U. and 1060 Å.U. replace their single term at 1127 Å.U. which is nearly the mean of these two. The justifications for their introduction lies in the work of Tousey, who has found (1) an absorption cut off at 1436 Å.U. exhibited by even thin slices, (2) a sharp, strong peak of selective reflection at 1190 Å.U. and a diffuse peak about 1060 Å.U., both remaining unchanged in wave-length and changing only slightly in intensity for different crystal orientations. The use of these terms with nearly equal strengths in place of the empirical term of Lowry and Coode-Adams extends the validity of the formulæ into the remote ultra-violet.

The third term at 310 Å.U. appears in the formulæ of Lowry and Coode-Adams and is unambiguously indicated to be necessary by the refraction data. Experiments have not advanced far enough into the ultra-violet to verify the existence of a specific maximum absorption at such a wave-length. Theoretically, however, the transitions of the L-electrons of silicon (with its neon-like core) to vacant outer levels would give rise to a term with a wave-length of about 200 Å.U. and the transitions of the L-electrons of oxygen to a term above 500 Å.U. The result would be to give a lumped effect *as if there were* an absorption at some intermediate wave-length. It will be noticed that the relative importance of the terms at λ 1190 and λ 1060 in the formulæ is approximately the same for the ordinary and extraordinary rays, but the relative importance of the term at λ 310 is distinctly less in the case of the extraordinary ray. The manner in which the birefringence alters with the frequency is influenced by this circumstance.

In the case of the ordinary ray the dielectric constant and the infra-red absorption frequencies have been taken without change from an old formula of Rubens which considers the lattice vibrations strongly active in respect of the ordinary ray (*viz.*, one at 21 μ, and three about 9 μ which have been lumped together into one term). A similar formula has been constructed by the author for the extraordinary index, taking into account the lattice oscillations strongly active for the extraordinary ray (namely one at 19 μ and two others near about 9 μ which have been lumped together). The appropriate value of the dielecttric constant and the oscillator strengths were determined from the refraction data.

The formula for optical activity was first designed to be *asymptotically equivalent to the Lowry and Coode-Adams formula* at long wave-lengths. The resulting large errors in the extreme ultra-violet were found to be removed by introducing a *square* term with a very small numerator, and with a characteristic wave-length below 1400 Å.U. This might be an effect of the continuous absorption below λ 1436, whose contribution to refraction is negligible. The constant 0·1905 appearing in the formula may possibly be the effect of a far-off infra-red term whose variation in the range of ·14 μ to 3 μ is negligible. The term at λ 310 is of less im-importance in optical activity than in refraction as is to be expected, since optical activity is more connected with the outer inter-atomic linkages than the inner structure.

3. Comparison with Facts*

(1) *The Ordinary Ray*

Wave-length (microns)	Refractive Index (Calculated)	Refractive Index (Observed)
0·185467	1·67589	1·67578
0·274867	1·58765	1·58752
0·396848	1·55812	1·55813
0·486133	1·54965	1·54968
0·587563	1·54423	1·54433
0·670786	1·54135	1·54147
0·794763	1·53835	1·53848
1·00	1·53489	1·53503
2·0582	1·51981	1·51998
3·000	1·49947	1·49962
4·09	1·4615	1·4620
5·0	1·410	1·417
7·0	1·095	1·167
33	2·39	2·53
52	2·22	2·23
63	2·19	2·19
83	2·167	2·15
∞	2·14	2·11

* Values of refractive indices and rotatory power above 0·185 μ are taken respectively from the treatises of Sosman and Lowry quoted before, Sosman's estimate of the more probable values of n_ω and n_e in air and at 18° C. being used. Data below 0·185 μ are taken from Servant's papers.

(2) *The Extra-ordinary Ray*

Wave-length (microns)	Refractive Index (Calculated)	Refractive Index (Observed)
0·185467	1·69007	1·68997
0·274867	1·59819	1·59813
0·396848	1·56776	1·56772
0·486133	1·55900	1·55898
0·587563	1·55343	1·55343
0·670786	1·55047	1·55048
0·794763	1·54741	1·54739
0·84467	1·54639	1·54640
1·0000	1·54381	1·54381
1·8000	1·53246	1·52342
2·0582	1·52814	1·52814
2·5000	1·5194	1·5195
3·0000	1·5070	1·5070
33	2·40	2·63
52	2·25	2·30
63	2·23	2·25
83	2·20	2·22
∞	2·175	2·15

(3) *Birefringence*

Wave-length (Microns)	n_ω (Calculated)	n_ϵ (Calculated)	$(n_\epsilon - n_\omega)\times 10^3$ (Calculated)	$(n_\epsilon - n_\omega)\times 10^3$ (Observed)
0·14546	1·85975	1·88365	23·90	23·64
0·15478	1·78722	1·80709	19·87	19·57
0·16619	1·73169	1·74863	16·94	16·72
6·17680	1·69703	1·71224	15·21	15·05

(4) *Optical Activity*

Wave-length (microns)	Calculated rotatory power (deg./mm.)	Observed rotatory power (deg./mm.)
0·1525	767	776
0·1550	722	724
0·1575	678·5	678·5
0·1625	600	599·5
0·1650	564·5	564·5
0·1675	533·5	533
0·1700	504	504·5
0·185398	371·3	370·9
0·198979	295·33	295·65
0·226909	200·5	200·9
0·232749	186·89	187·247
0·273955	121·72	122·123
0·3693999	60·019	60·058
0·435834	41·534	41·551
0·520908	28·237	28·245
0·579066	22·5425	22·5465
0·6707846	16·536	16·5359
1·342	3·857	3·894
1·480	3·132	3·168
2·400	1·073	1·074
3·210	0·512	0·520

4. Discussion

The formulæ proposed are valid with fair accuracy over the whole range of measurements, while the older formulæ, highly accurate up to the near ultra-violet, fail badly in the remote ultra-violet. The following tables (the first one taken from Servant's paper on the birefringence) illustrate the deviations of the older formulæ.

Wave-length (Å.U.) ..	2210	2099	1932	1515	1454
$(n_e - n_\omega) \times 10^3$ observed ..	11·97	12·45	13·46	20·72	23·64
$(n_e - n_\omega) \times 10^3$ calculated from Coode-Adam's formulæ	11·96	12·41	13·32	18·59	20·32

Wave-length ..	λ 2174	λ 1700	λ 1550
Observed ρ ..	226·91	504·5	724
ρ Calculated from Lowry Coode-Adams-formula	226·98	509·5	748

This progressive error is almost completely annulled in the formulæ proposed by the author and this suggests that the changes he has made are at least in the right direction. The wave-lengths λ 1190 and λ 1060 are known correct only to 10 Å.U., and the employment of more precise values, when these are secured by experiment, might improve the fit.

I voice here my gratitude to Sir C. V. Raman for suggesting the problem and his interest in the investigation.

5. Summary

New formulæ using the latest data available and based on the observed spectroscopic behaviour of quartz have been given for the refraction and optical activity of quartz, which fit the facts over a wider range of frequencies than any formula proposed so far.

Appendix

The older formulæ from which the present ones have sprung are set out below:—

Rubens' formula for the ordinary ray:—

$$n_\omega^2 = 4{\cdot}57877 + \frac{0{\cdot}0010654}{\lambda^2 - 0{\cdot}010627} + \frac{44{\cdot}224}{\lambda^2 - 78{\cdot}22} + \frac{713{\cdot}55}{\lambda^2 - 430{\cdot}55}$$

Coode-Adams' for the ordinary and extraordinary rays:—

$$n_\omega^2 = 3{\cdot}53445 + \frac{0{\cdot}008067}{\lambda^2 - 0{\cdot}0127493} + \frac{0{\cdot}002682}{\lambda^2 - 0{\cdot}000974} + \frac{127{\cdot}2}{\lambda^2 - 108}$$

$$n_\epsilon^2 = 3{\cdot}5612557 + \frac{0{\cdot}00844614}{\lambda^2 - 0{\cdot}0127493} + \frac{0{\cdot}00276113}{\lambda^2 - 0{\cdot}000974} + \frac{127{\cdot}2}{\lambda^2 - 108}$$

Lowry and Coode-Adams' formula for optical activity:—

$$\rho = \frac{9{\cdot}5639}{\lambda^2 - 0{\cdot}0127493} - \frac{2{\cdot}3114}{\lambda^2 - 0{\cdot}000974} - 0{\cdot}1905$$

6. References

Sosman	..	*The Properties of Silica* (Amercian Chemical Society, 1927).
Lowry	..	*Optical Rotatory Power* (Longman's, 1935).
—— & Coode-Adams		*Phil. Trans. Roy. Soc.*, 1927, **226** A.
Coode-Adams	..	*Proc. Roy. Soc.*, 1928, **117** A.
	..	*Ibid.*, 1928, **121** A.
Servant	..	*Comptes Rend.*, 1936, **202.**
	..	*Ibid.*, 1937, **205.**
	..	*Ibid.*, 1938, **207.**
Duclaux and Jeantet	..	*J. de Physique.* I (III), 1926.
Tousey	..	*Phys. Rev.*, 1940, **57.**
Rubens	..	*Ann. der Phys. und Chemie.*, 1897, **60.**
Saxena	..	*Proc. Ind. Acad. Sci.*, 1940, **12** A.

THERMO-OPTIC BEHAVIOUR OF SOLIDS

I. Diamond

By G. N. Ramachandran

(From the Department of Physics, Indian Institute of Science, Bangalore)

Received January 29, 1947

(Communicated by Sir C. V. Raman, Kt., F.R.S., N.L.)

1. Introduction

A study of the temperature-variation of the refractive indices of solids is interesting from many points of view. On the experimental side, optical measurements are capable of very high precision and thus it is possible to obtain accurate data. Theoretically, a satisfactory theory of the variation has not been forthcoming so far. In fact, it is found that many crystals like rocksalt, fluorspar and quartz exhibit a diminution of their refractive indices for visible light on heating, while others like diamond (Sella, 1891) and zinc-blende (Maria Mell, 1923) show an increase. Also, some of the crystals of the former type show the reverse type of behaviour, namely an increase in the refractive index with temperature, in the extreme ultra-violet. An adequate theory of the phenomenon must be capable of explaining all these facts.

The experimental methods of measurement are also capable of improvement. The usual procedure in finding the variation of refractive index with temperature (dn/dt) is to determine the absolute index (n) at various temperatures and then to deduce dn/dt from these measurements. It would, of course, be much more accurate if one could devise a method in which dn/dt is directly measured as a function of temperature. Such a method has been designed by the author and is discussed fully in a later section of this paper. The method has been applied to the case of diamond and dn/dt has been measured over the range of temperatures from $-180°$ C. to $+450°$ C. for three wavelengths in the visible region.

A phenomenological theory of the temperature-variation of the refractive index has also been developed in this paper. It is based on the idea that the refractive index can be expressed in terms of the number of dispersion centres per unit volume and the polarisabilities of these centres. The latter again is dependent on the dispersion frequencies of the system. The variation in the refractive index of the solid can thus be represented

by two terms, one arising from the change in the number of dispersion centres and another from the variation in the spectral position of the dispersion frequencies. The idea is applied to the case of diamond in this paper and it is shown that the rate of change of the dispersion frequencies with temperature is correlated to the rate of change of other electronic and lattice frequencies observed for the crystal. The application of the formulæ to the case of fused silica enables one to calculate dn/dt over the whole spectral range, which are found to fit remarkably well with the experimental data. This will be reported in Part II of these series.

2. Experimental Procedure

The principle of the method may be described as follows. One employs a plate of thickness l and obtains interference fringes by the light obtained from the two surfaces of the plate at normal incidence. (Either the transmitted or the reflected system may be employed.) The path difference between the two interfering beams is $x = 2nl$, where n is the refractive index. Suppose one measures the change in this path, Δx for a known change of temperature Δt. Then,

$$\Delta x/\Delta t = 2n.\ \Delta l/\Delta t + 2l.\ \Delta n/\Delta t,$$

so that

$$\frac{\Delta n}{\Delta t} = \frac{1}{2l} \cdot \frac{\Delta x}{\Delta t} - n \cdot \frac{1}{l}\frac{\Delta l}{\Delta t}$$

$$= (1/2l)\,(\Delta x/\Delta t) - n\alpha, \qquad (1)$$

where α is the coefficient of linear expansion at temperature t. Thus, if α is known, then by measuring Δx and Δt, dn/dt can be accurately obtained. Of course, n has also to be known, but only to 3 significant figures for getting an accuracy of 1% and not 5 or 6 significant figures as are necessary with the usual prism methods. Another advantage of the interference methods is that the value of dn/dt obtained is for the absolute refractive index and that no corrections are required for the change in the index of air as is necessary with the prism methods.

In practice, two types of experimental arrangement can be visualised employing the above principle, one or the other being suitable for a particular case. Suppose that one is able to obtain plane-parallel plates of the specimen, as is for instance possible with mica. It is best in this case to form Haidinger rings with monochromatic light with the plate kept in a suitable furnace. When heated, the rings expand or contract and a measurement of the expansion or contraction gives one the alteration in path. One method of obtaining $\Delta x/\Delta t$ is to accurately measure Δx for

a known difference of temperature Δt. But if one is interested in measuring dn/dt over a whole range of temperatures it is much more convenient to make a continuous observation. The temperature of the furnace is raised steadily at a very slow rate and the temperature corresponding to the passage of successive fringes across a fiduciary cross-wire can be noted.

If optically parallel plates are not available, another method can be used, which was in fact employed with diamond in the present experiment. The crystal used for the purpose was N.C. 73 from the collection of Sir C. V. Raman, which was a rectangular plate with a thickness of 0·670 mm. The surfaces of the plate were deposited with a thin layer of aluminium by the evaporation process in order to increase the reflecting power. When viewed by transmission in a parallel beam of monochromatic light, localised interference fringes were observed, which consisted of sharp bright almost circular rings. These were produced because of the variations in the thickness of the specimen. A fine line on the surface of the crystal formed a reference mark across which the fringes shifted as the crystal was heated. It may be mentioned that this method of observation is the same as was employed by the author in determining variations of the absolute path of a ray of light through the crystal plate for calculating the photo-elastic constants of diamond (Ramachandran, 1947).

The diamond was kept in a suitable furnace and the fringes were observed by means of a microscope. The continuous observation method mentioned in connection with the Haidinger rings was employed with these fringes also. The rate of heating was so slow that it took 6 hours to heat the crystal from room temperature to 400° C. The temperature was measured by a standardised thermocouple and the readings of the measuring instrument were such that an accuracy of $\pm 1°$ C. could be obtained even at the highest temperatures. The experiments were performed with three different wavelengths, *viz.*, the 4358 and 5461 Å.U. radiations of the mercury arc and the yellow radiations of 5893 Å.U. from the sodium lamp. In the first case, more than 40 fringes shifted across the reference mark in heating from room temperature to 400° C. and in the last, nearly 30. The observations were repeated with the cooling crystal, this also taking roughly 6 hours. The temperature readings taken during heating and cooling never differed by more than one unit in the last decimel place, *i.e.*, nearly 1° near about 400° C. and less at lower temperatures. For each wavelength, the experiments were also repeated reversing the positions of the source of light and of the observing microscope. This was done in order to correct for any movement of the crystal or of the whole furnace due to heating. Actually, no difference could be noticed between the two readings. Six

independent experiments were performed with each wavelength and the finally calculated values were the means of these.

The values of α at various temperatures were available from the measurements of R. S. Krishnan (1946 *a*). Knowing Δt corresponding to each wavelength shift, dn/dt was calculated for the mean temperature t. When these values were plotted and a smooth curve drawn through them, it was found that the points appreciably diverged from the mean. This was obviously due to the restricted accuracy of the temperature measurement. Consequently, the values of dn/dt were later calculated from the temperature difference corresponding to a shift of 3, 4 or 5 fringes. These fell very well on a smooth curve, as will be seen from the curves reproduced in Fig. 1. Here, the continuous curves represent the mean value of all the experiments for each wavelength. The points denote the values from a single experiment calculated in the above manner.

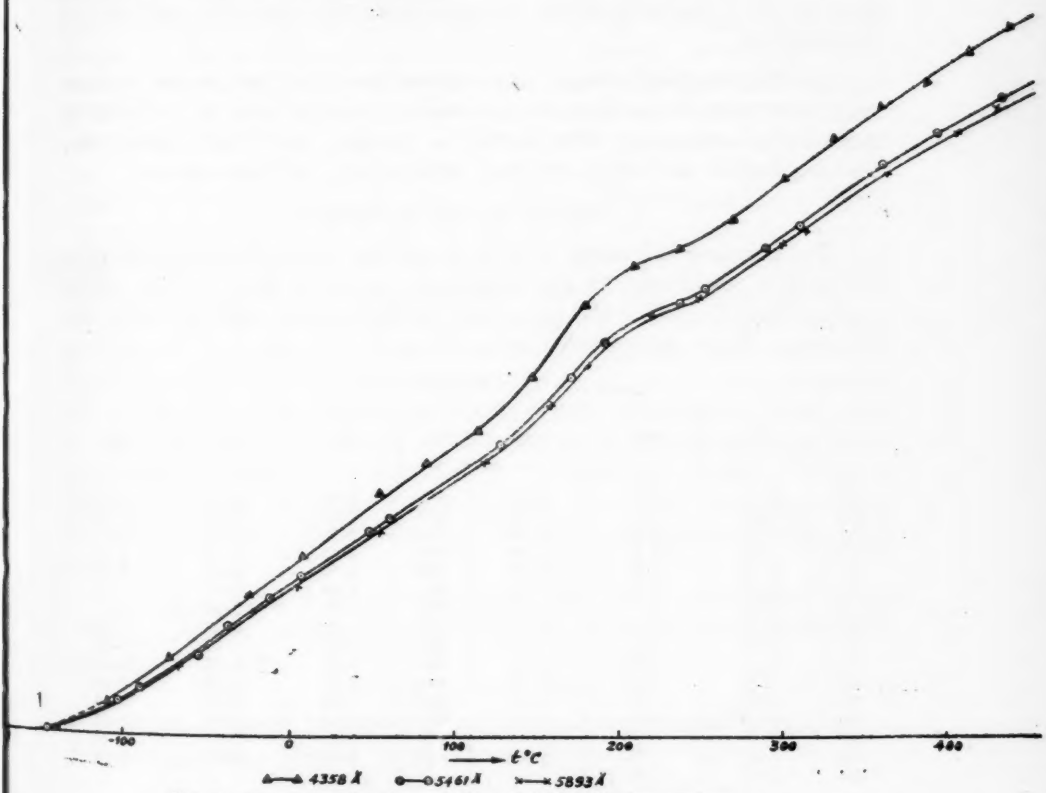

FIG. 1. Curves showing the variation of dn/dt with temperature.

The measurement of dn/dt was also made for temperatures down to — 180° C. Here, the accuracy was not as high as at higher temperatures, since the rate of variation was small and only 4 fringes shifted over the whole range and also since measurement could be made only during warming and not during cooling. dn/dt was calculated from the temperature difference for the shift of one fringe at a time. The crystal was kept in a copper block which was screwed on to the bottom of a brass tube in which was kept liquid air. The tube with the crystal was enclosed in an outer jacket of glass and the intervening space was kept evacuated. The thermocouple was kept in intimate contact with the bottom of the brass tube. The whole arrangement was first cooled to the temperature of liquid air and then allowed to warm up. It took nearly 3 hours for the system to attain the room temperature. During this period, temperatures were measured corresponding to the passage of each fringe across the reference mark. It was noticed that upto about — 150° C. or so there was no shift at all of the fringes, showing that the rate of variation of the refractive index was extremely small at these temperatures.

An obvious disadvantage of the method described here is that it is not very convenient for work in the ultra-violet; but this may be remedied by the use of photography. The method is, however, particularly useful when one requires to find *dn/dt accurately over a range of temperatures.*

3. Results of the Experiment

The experimental values of dn/dt at various temperatures for the three wavelengths are shown by the continuous curves in Fig. 1. The values read off from these ($\times 10^5$) are shown in Table I and will be useful for reference. These are probably accurate to 1%.

Table I

t° C.	4358	5461	5893	t° C.	4358	5461	5893
−150	0·02	0·01	0·01	160	2·33	2·04	2·00
−140	0·03	0·03	0·03	180	2·60	2·26	2·22
−120	0·13	0·10	0·09	200	2·78	2·45	2·41
−100	0·24	0·21	0·19	220	2·88	2·57	2·53
− 80	0·38	0·32	0·30	240	2·96	2·66	2·62
− 60	0·53	0·45	0·43	260	3·06	2·76	2·72
− 40	0·68	0·59	0·57	280	3·20	2·88	2·84
− 20	0·83	0·73	0·70	300	3·35	3·03	2·98
0	0·99	0·87	0·84	320	3·50	3·17	3·12
20	1·14	1·01	0·98	340	3·65	3·30	3·25
40	1·29	1·15	1·12	360	3·80	3·43	3·38
60	1·44	1·29	1·26	380	3·94	3·56	3·50
80	1·59	1·43	1·40	400	4·08	3·68	3·62
100	1·75	1·57	1·54	420	4·20	3·80	3·74
120	1·91	1·71	1·68	440	4·31	3·91	3·84
140	2·07	1·85	1·82				

The most interesting fact that comes out of the investigation is that dn/dt is positive for diamond over the whole range of temperatures. This has been observed by Sella (*loc. cit.*) from room temperature to 90° C. His value of $+1{\cdot}86 \times 10^{-5}$ for a mean temperature of 50° C. and 5893 Å.U. is however too large, the present experiment indicating a value of about $+1{\cdot}20 \times 10^{-5}$. It is found that dn/dt is extremely small for temperatures below − 150° C. and that it increases practically linearly with temperature from about − 100° to 450° C. However, a slight hump is observed in the graph of dn/dt *vs.* t in the neighbourhood of 210° C., as may be seen from Fig. 1. Very accurate and repeated sets of readings have been taken in this range of temperatures and it has been verified that the hump is a genuine effect. The deviation of dn/dt is however only of the order of 10%. In fact when the values of n calculated from the data for dn/dt are plotted against t, it is practically impossible to detect the kink in the curve, even when plotted on a highly magnified scale. The author is not in a position to give a definite explanation for the hump at 210° C. It may however be pointed out that a similar variation, though in a much more pronounced manner, is shown by the refractive index of fused silica in the neighbourhood of 575° C., the temperature of $\alpha-\beta$ transformation of quartz. Here, the kink is observable in the graph of refractive index against temperature. It is not clear what kind of transformation, if any, occurs in diamond near about 200° C. It has however been observed (Chandrasekharan, 1946) that diamond exhibits very bright thermoluminescence at about this temperature. Similarly, Nayar (1941) found that the intensity of luminescence diminishes rapidly at these temperatures and practically vanishes at 300° C. The particular diamond that was studied exhibited a feeble blue luminescence. It would be interesting to repeat the dn/dt measurements with highly luminescent and non-luminescent diamonds to discover if the magnitude of the hump has any relation to luminescence. Another interesting fact is that a particularly low value for the Raman frequency of diamond has been observed near this temperature (R. S. Krishnan, 1946*b*). In Fig. 1 of this reference, it will be noticed that the two values at temperatures 213° C. and 242° C. fall well below the continuous curve through the other points.

Leaving aside such minor differences, it has been calculated that the refractive index of diamond n_t at temperature t can be represented by a formula of the type

$$n_t = n_0(1 + \alpha t + \beta t^2) \qquad (2)$$

from about − 100° C. to 400° C. The values of α and β for the three wavelengths studied are given in Table II.

TABLE II

Wavelength Å. U.	$\alpha \times 10^6$	$\beta \times 10^6$
4358	9·9	7·8
5461	8·7	7·0
5893	8·4	7·0

4. THEORY OF THE THERMAL VARIATION OF REFRACTIVE INDEX

Pockels (1902) has recognized that the rate of change of refractive index with temperature (dn/dt) can be divided into two parts, namely, a pure temperature change which we may denote by $\partial n/\partial t$ and another part due to the change in density which accompanies the temperature change, $(\partial n/\partial \rho)_t \cdot d\rho/dt$. Thus,

$$\frac{dn}{dt} = \left(\frac{\partial n}{\partial \rho}\right)_t \cdot \frac{d\rho}{dt} + \left(\frac{\partial n}{\partial t}\right)_\rho = \mathrm{A} + \mathrm{B} \text{ say} \tag{3}$$

Of these, the quantity A may be calculated from photo-elastic data. For a cubic crystal,

$$\mathrm{A} = -\frac{2}{n^3} \cdot \frac{(p_{11} + 2p_{12})}{3} \cdot \gamma, \tag{4}$$

where γ is the coefficient of cubic expansion and p_{11} and p_{12} are the elasto-optic constants. The same relation is true for isotropic solids like glasses, while similar relations hold for crystals of other classes. When A is actually calculated in this manner, it is found that it is not in general equal to dn/dt. Pockels, in the paper cited above, has shown that A is always algebraically less than dn/dt so that B is a positive quantity for a number of glasses of varying composition. In Table III below, dn/dt, A and B are given for a number of crystals. The data have been collected from the *Handbuch der Physik*, Vol. XXI, 1929, Ch. 19, except for diamond for which the data are taken from a paper by the author (1947).

TABLE III

Substance	$dn/dt \cdot 10^6$	$A \cdot 10^6$	$B \cdot 10^6$
Rocksalt ..	−37·4	−37·2	− 0·2
Fluorspar ..	−12·1	−13·5	+ 1·4
Quartz-ord ..	− 6·50	−12·80	+ 6·30
,, -ext ..	− 7·54	−14·10	+ 6·56
Calcite-ord ..	+ 0·69	− 8·9	+ 9·6
,, -ext ..	+10·57	− 1·9	+12·5
Topaz-α ..	+ 8·1	− 0·38	+ 8·5
,, -β ..	+ 9·0	− 0·713	+ 9·7
,, -γ ..	+ 8·0	− 0·684	+ 8·7
Diamond ..	+10·5	+ 3·8	+ 6·7

It will be seen that, in all the cases except rocksalt, B is positive. Even for rocksalt one cannot say that the negative value, which is less than 1% of the observed *dn/dt* is not spurious. We may thus say that, in general, *crystals and glasses exhibit a pure thermal coefficient of variation of refractive index which is positive.*

This picture does not however go deep enough into the problem except for separating the density and temperature effects. In fact, one can give a quantitative theory of the thermo-optic behaviour by considering the dispersion of solids and its origin. It has been the attempt of many workers to fit the dispersion data of solids into a formula of one of the following types:—

$$n^2 = C' + \sum_r A_r/(\lambda^2 - \lambda_r^2) - K\lambda^2 \qquad (5)$$

$$n^2 = C + \sum_r B_r \lambda^2/(\lambda^2 - \lambda_r^2) - K\lambda^2 \qquad (6)$$

where the term $K\lambda^2$ may sometimes be absent. These two forms are really equivalent and can be converted one into the other by merely changing the constants. Also, the last term arises from the presence of an infra-red frequency or frequencies whose positions are not known, so that in general we may write (6) in the form

$$n^2 = C + \sum_r a_r \lambda^2 \lambda^2_r/(\lambda^2 - \lambda^2) = C + \sum_r a_r/(\bar{\nu}_r^2 - \bar{\nu}^2) \qquad (7)$$

where $\bar{\nu}$ is the wave number of a radiation of wavelength λ. Now, the Ketteler-Helmholtz theory (and also the more recent Kramers-Heisenberg theory) of dispersion leads to a formula of the type

$$n^2 = 1 + \sum_r a_r/(\bar{\nu}_r^2 - \bar{\nu}^2) \qquad (8)$$

where all the dispersion frequencies are taken into account. Usually, the empirical formula is derived from observations in the ultra-violet, visible and infra-red regions of the spectrum. If there is a dispersion frequency in the remote ultra-violet, it will contribute a constant term to the right-hand side of the formula, which will then be of the type (7). We shall, however, consider only a formula of the type (8) in our theory since it is of the most general type. It is obvious that the quantities a_r in the numerator are proportional to the number of dispersion centres per unit volume and to the oscillator strength of each centre.

Now, if such a formula is true for a particular temperature, then a similar formula with slightly different constants must hold for a slightly different temperature, so that one can obtain an expression for *dn/dt* by

differentiating these expressions with respect to t. One thus obtains from (8)

$$2n\frac{dn}{dt} = \sum_r \left[-\frac{2a_r \bar{\nu}_r}{(\bar{\nu}_r^2 - \bar{\nu}^2)^2}\frac{d\nu_r}{dt} + \frac{1}{(\bar{\nu}_r^2 - \bar{\nu}^2)} \cdot \frac{da_r}{dt} \right] \tag{9}$$

Since a_r is proportional to ρ, the density of the substance, $da_r/dt = (a_r/\rho)$. $(d\rho/dt) = -a\gamma$, where γ the coefficient of cubical expansion.* Thus, the second term in the right-hand side of (9) becomes

$$\sum_r -\gamma \cdot a_r/(\bar{\nu}_r^2 - \bar{\nu}^2) = -\gamma(n^2 - 1) \qquad \text{from (8).}$$

$$\frac{dn}{dt} = -\frac{\gamma(n^2-1)}{2n} - \frac{1}{n}\sum_r \frac{a_r \bar{\nu}_r}{(\bar{\nu}_r^2 - \bar{\nu}^2)} \cdot \frac{d\bar{\nu}_r}{dt} \tag{10}$$

This is a general expression for dn/dt in terms of known constants of the substance. $\bar{\nu}_r$ is known from the dispersion formula, but $d\bar{\nu}_r/dt$ is not known in many cases. But it may be calculated from the values of dn/dt for a particular wavelength and then formula (10) can be verified to hold over the whole range of wavelengths. It will be convenient to express $d\bar{\nu}_r/dt$ in the form $-\chi_r \bar{\nu}_r$, where χ_r is just a constant expressing the rate of change of wavenumber as so many per wavenumber of the dispersion frequency. It may be noted that χ_r is also equal to $(1/\lambda_r)(d\lambda_r/dt)$. Then,

$$\left.\begin{aligned} \frac{dn}{dt} &= -\frac{\gamma(n^2-1)}{2n} + \frac{1}{n}\sum_r \frac{a_r \bar{\nu}_r^2}{(\bar{\nu}_r^2 - \bar{\nu}^2)^2}\chi_r \\ &= -\frac{\gamma(n^2-1)}{2n} + \frac{1}{n}\sum_r \frac{a_r \lambda^4 \lambda_r^2}{(\lambda^2 - \lambda_r^2)^2}\chi_r \end{aligned}\right\} \tag{11}$$

In this expression, dn/dt has been split up into two parts, one due to a change in the number of dispersion centres per unit volume and another due to the changes in the dispersion frequencies. We may denote these by P and X respectively. The term X arises from the change in the dispersion frequency with temperature; but it is not at all necessary that this change should be a pure temperature effect. It is necessary to distinguish between the change that is produced by the accompanying change in volume (or density) and the change due to temperature alone. In symbols,

$$\begin{aligned} \mathrm{X} &= \frac{\partial n}{\partial \bar{\nu}} \cdot \frac{\partial \bar{\nu}}{\partial v} \cdot \frac{\partial v}{\partial t} + \frac{\partial n}{\partial \bar{\nu}} \cdot \frac{\partial \bar{\nu}}{\partial t} \\ &= \mathrm{Q} + \mathrm{R} \text{ (say)} \end{aligned} \tag{12}$$

Obviously, P arises completely from the change in density, so that one gets immediately,

$$\mathrm{A} = \mathrm{P} + \mathrm{Q}, \qquad \mathrm{B} = \mathrm{R} \tag{13}$$

* This implies the assumption that the oscillator strengths, *i.e.*, the transition probabilities of the dispersion centres, do not alter with temperature.

These considerations are, of course, purely formal, but they are yet interesting. It is seen that one has to take into account a possible shift of the dispersion frequencies even to explain the alteration of refractive index with pressure. The shift of the frequencies with pressure is not negligible. In fact, for diamond at 25° C. and 5893 Å.U., we have from (11) $P = -3{\cdot}1 \times 10^{-6}$ and combining this with the data in Table I, we have

$$P = -3{\cdot}1 \times 10^{-6},\ Q = +6{\cdot}9 \times 10^{-6},\ R = +6{\cdot}7 \times 10^{-6} \qquad (14)$$

Here, the shift in frequency, due to the change in volume is as much as that due purely to change of temperature.

The considerations put forward above refer strictly only to the behaviour of cubic crystals or of isotropic bodies. In other crystals, the linear thermal expansion is not the same in all directions and the refractive indices in different directions are influenced differently. We shall not go into these questions in this paper.

5. Discussion of the Results obtained with Diamond

We shall now apply the considerations put forward in the previous section to the case of diamond. The dispersion of diamond can be represented by the formula

$$n^2 - 1 = \sum_{1,2} \frac{a_r \lambda_r^2 \lambda^2}{\lambda^2 - \lambda_r^2} \left.\begin{array}{l} a_1 = 3{\cdot}859 \times 10^{10},\ a_2 = 1{\cdot}080 \times 10^{9} \\ \lambda_1 = 1060\ \text{Å.U.},\quad \lambda_2 = 1750\ \text{Å.U.} \end{array}\right\} \qquad (15)$$

(Peter, 1923). Consequently, dn/dt is given by Eq. (11). It will be noticed that both the dispersion frequencies are in the extreme ultra-violet and that one of them at 1060 Å.U. is nearly 40 times as strong as the other at 1750 Å.U. We shall make the assumption that $\chi_1 = \chi_2$, in other words that both of them vary in proportion to their frequencies. It will be seen presently that this assumption is not unjustified. Besides, since λ_2 is very weak, slight differences in the value of χ_2 will not matter. Thus, putting $\chi_1 = \chi_2 = \chi$ its value calculated from the measurements of dn/dt for the green and yellow radiations comes out to be $7{\cdot}6 \times 10^{-6}$ at 50° C. It is interesting to note that this is of the same order as the value of χ for the fundamental lattice vibration of 1332 cm.$^{-1}$. From the data of R. S. Krishnan (1946 *b*), it has been calculated that χ at 50° C. is $9{\cdot}8 \times 10^{-6}$ for this frequency. It is thus found that the rate of variation of the ultra-violet dispersion frequencies is nearly the same as that of the lattice frequency in the infra-red provided the rate is taken as so many wave-numbers per wave-number per degree. In fact, this behaviour is exhibited by practically all the electronic lines found in the absorption and emission spectrum of diamond. In Table III the wavelengths of various such lines are given both at liquid air and room

temperatures and the total change is calculated and given as so many wavenumbers per 1000 wavenumbers (1000 $\Delta \bar{\nu}/\bar{\nu}$) in the third column.

TABLE IV

λ at liquid air temperature	λ at room temperature	1000 $\Delta\bar{\nu}/\bar{\nu}$	Reference
Disperson	Frequencies	0·6	This paper
2306	2308	0·9	K. G. Ramanathan (1946)
2309	2312	1·3	
2355·9	2359	1·3	
2360	2364	1·8	
3034	3037	1·0	Robertson, Fox and Martin (1934)
3064	3067	1·0	
3154	3157	1·0	
3201	3204	1·0	
3298	3302	1·3	
3447	3450	0·83	A. Mani (1944)
4152	4156	0·83	
5032	5038	1·2	
5115	5123	1·6	
5198	5204	1·2	
5286	5292	1·1	
5359	5367	1·5	
5451	5455	0·7	
5695	5701	1·0	
5758	5768	1·7	
1333·2cm.$^{-1}$	1331·8cm.$^{-1}$	1·1	R. S. Krishnan (1946 *b*)

The approximate constancy of the numbers in the third column is significant. It shows that the behaviour of the electronic lines is similar to that of the lattice frequency. This is not surprising when one remembers that the electronic lines arise from transitions of the very electrons that are responsible for the binding forces in the lattice.

The refractive indices at various temperatures were calculated from the data for dn/dt by numerical integration assuming the values at 20° C. given by Peter (*loc. cit.*). In Fig. 2 the course of the refractive index-temperature curve has been plotted from these calculations. It will be noticed that the refractive index does not at all change at very low temperatures. In fact below — 100°, the change does not even amount to one unit in the fourth decimel place, which is the accuracy to which absolute indices are known. Extrapolating to the absolute zero and taking Peter's value for the refractive indices at 20° C., the indices at absolute zero for the three wavelengths have been calculated to be

2·4490 at λ 4358, 2·4225 at λ 5461, 2·4165 at λ 5893.

An attempt was made to calculate the course of the refractive index-temperature curves, assuming that the dispersion frequencies vary in the

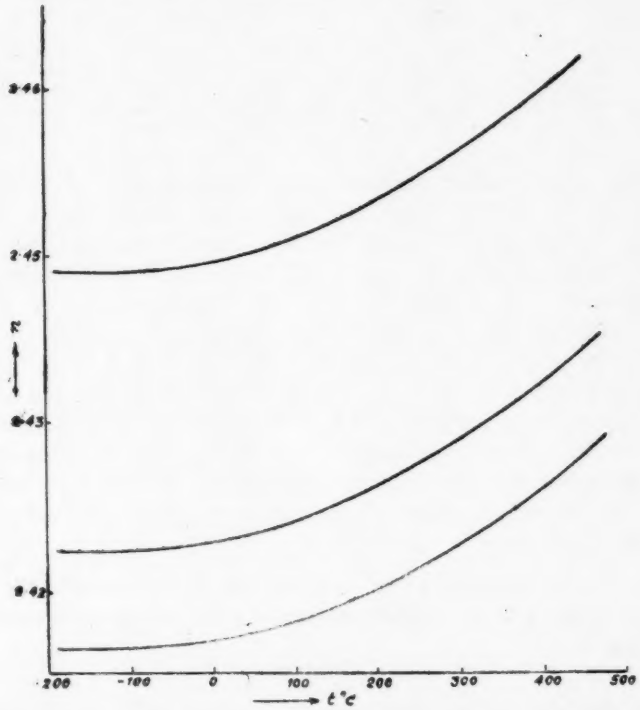

FIG. 2. The variation of refractive index of diamond with temperature. The three curves are from top to bottom for wavelengths 4358, 5461 and 5893 Å.U. respectively.

same way as (*a*) the lattice frequency or (*b*) the electronic line at 4152 Å.U. Data for the temperature variation of these are available from R. S. Krishnan (1946 *b*) and P. G. N. Nayar (1941) respectively. The experimental values of $(n_t - n_{25})$ are shown along with those calculated from assumptions (*a*) and (*b*) in Table V below. It will be seen that although the general trend of the curve is shown by the calculated values, the numerical agreement with experiment is not very satisfactory. This only shows that the variation with temperature of the dispersion frequency does not exactly follow that of the lattice frequency or the other electronic frequency at 4152 Å.U. although it is of the same order.

TABLE V

Temperature °C.	−180	25	100	200	300	400
$n_t - n_{25}$ (Exp.) ..	−0·0008	0	+0·0009	+0·0026	+0·0055	+0·0098
do from (*a*) ..	−0·0021	0	+0·0015	+0·0038	+0·0063	+0·0082
do from (*b*) ..	−0·0014	0	+0·0017	+0·0052	..	..

It was mentioned above that χ was found to be $7{\cdot}6 \times 10^{-6}$ at 50° C. A recalculation of dn/dt from this value of χ showed that it fitted with experimental values for 5893 and 5461 Å.U., but was too small for 4358 Å.U. The calculated values were 1·20, 1·22 and $1{\cdot}27 \times 10^{-6}$, while experiment gave values of 1·19, 1·22 and $1{\cdot}36 \times 10^{-6}$ respectively for the three wavelengths. The author is of the opinion that the discrepancy for 4358 Å.U. is due to the presence of a weak absorption at 4156 Å.U. in the diamond. It may be pointed out that on account of its proximity, the contribution to dn/dt by this frequency at 4358 Å.U. is nearly 20 times those at 5461 and 5893 Å.U. It will be interesting to see whether the discrepancy is larger with a diamond having a stronger absorption at 4156 Å.U. and also to actually detect the presence of anomalous dispersion of refractive index near this wavelength.

My sincere thanks are due to Prof. Sir C. V. Raman for the kind interest that he took in the investigation and for the many discussions I had with him.

SUMMARY

A phenomenological theory has been put forward for the variation of the refractive indices of solids with temperature, based on the idea that the refractive index can be expressed in terms of the number of dispersion centres and the polarizabilities of these centres, which are again dependent on the dispersion frequencies. The refractive index variation can then be represented as the sum of two terms, one arising from the change in the number of dispersion centres and the other from the variation of the frequencies. Accurate data of the thermal variation of the refractive index of diamond have been obtained for the first time from − 180° C. to 450° C. for three wavelengths, 4358, 5461 and 5893 Å.U. A new method was employed for this purpose which measures dn/dt directly and is capable of general application. When applied to diamond, the theoretical ideas bring out the interesting fact that the rate of change of the dispersion frequencies with temperature is correlated to the rate of change of the fundamental lattice frequency of the crystal.

References

1. Chandrasekharan, V. .. *Proc. Ind. Acad. Sci.* A., 1946, **24**, 187.
2. Krishnan, R. S. .. *Ibid.*, 1946 *a*, **24**, 33.
3. ———— .. *Ibid.*, 1946 *b*, **24**, 45.
4. Mani, A. .. *Ibid.*, 1944, **19**, 231.
5. Maria Mell .. *Zeits. f. Phys.*, 1923, **16**, 224.
6. Peter, F. .. *Ibid.*, 1923, **15**, 358.
7. Pockels, F. .. *Ann. d. Phys.*, 1902, **7**, 745.
8. Ramachandran, G. N. .. *Proc. Ind. Acad. Sci.* A., 1947, **25**, 208.
9. Ramanathan, K. G. .. *Ibid.*, 1946, **24**, 137.
10. Robertson, Fox & Martin .. *Phil. Trans. Roy. Soc.* A, 1934, **232**, 482.
11. Sella, A. .. *Rend. Acad. Lincei.*, 1891, **7**, 300.
    See Zeits. f. Krist., 1894, **23**, 193.
12. Nayar, P. G. N. .. *Proc. Ind. Acad. Sci.* A, 1941, **13**, 284.

THERMO-OPTIC BEHAVIOUR OF SOLIDS

II. Fused Quartz

By G. N. Ramachandran

(From the Department of Physics, Indian Institute of Science, Bangalore)

Received February 5, 1947

(Communicated by Sir C. V. Raman, Kt., F.R.S., N.L.)

1. Introduction

In Part I of these series, some general considerations were put forward indicating how a phenomenological theory can be developed for the variation of refractive indices of solid substances with temperature. In this paper, a quantitative application of the theory is made to the case of fused quartz. It is shown that the theory can account satisfactorily for the variation of the refractive index with temperature over the whole spectral range from the extreme ultra-violet up to the red, and also for the course of the refractive index-temperature curve for a particular wavelength.

Fused quartz is particularly interesting in these studies because its thermal coefficient of expansion is extremely small. As is well known, the density of quartz falls down on fusing, but thereafter, it undergoes very little change with temperature when the virteous silica is heated or cooled. Consequently, the variation of refractive index with temperature is mainly caused by the variation in the dispersion frequencies, the contribution due to the variation in the number of dispersion centres being comparatively small. On the analogy of the result obtained with diamond, one may assume that the dispersion frequencies of silica also move to increasing wavelengths with rise of temperature. This has in fact been verified for the lattice frequencies (Nedungadi, 1940). Then, the contribution to dn/dt by this cause is positive and since the volume change is small, the negative contribution to dn/dt from this cause will be much smaller than the positive component. Consequently, one would expect that vitreous silica would exhibit a resultant positive dn/dt. This is in fact found to be the case over the whole spectrum (Sosman, 1927).

In crystalline quartz, on the other hand, the thermal expansion is appreciable, and there is the possibility of the negative component of dn/dt being the larger one. In fact, both the ordinary and extraordinary indices

of α-quartz diminish with rise of temperature in the visible and near ultra-violet (Sosman, *loc. cit.*). In the far ultra-violet they increase with rise of temperature, since the positive component of dn/dt becomes large owing to the approach to the dispersion frequencies.

2. Calculation of the Thermal Variation of Refractive Index for Different Wavelengths

The dispersion of vitreous silica has been studied by Martens and Micheli (1904) who have fitted their data to the following formula with one dispersion frequency in the ultra-violet:

$$n^2 = 1{\cdot}36112 + 0{\cdot}74655\,\lambda^2/\lambda^2 - (0{\cdot}107044)^2 - 0{\cdot}01350\lambda^2 \qquad (1)$$

the wavelength being expressed in microns. The author has verified that this formula fits the refractive index data from 1850 Å.U. to 6500 Å.U. It may be noticed that the dispersion frequency is at 1070 Å.U., which is very close to that used for crystalline quartz by other workers (Coode-Adams, 1928; Radhakrishnan, 1947). In the work of Radhakrishnan, two frequencies at 1060 Å.U. and 1190 Å.U. are employed, the latter being much weaker. These frequencies have actually been observed for quartz by Tousey (1940) as reflection maxima analogous to the *Reststrahlen* in the infra-red. For fused quartz, Tousey (*loc. cit.*) found two bands in very nearly the same positions as for crystalline quartz, but very much broader. Considering the relative strengths of the two frequencies, the representation of their total effect at regions of the spectrum not close to them by a single term employing a frequency of 1070 Å.U. appears justifiable. The infra-red term in the above formula (1) is represented by a term of the type $-K\lambda^2$ and does not explicitly involve the frequency. However, there are reasons to believe that none of the frequencies in the infra-red are nearer than 8μ. In the dispersion formula of quartz (Rubens and Nichols, 1897; Radhakrishnan, *loc. cit.*), there is a weak term with the dispersion wavelength in the neighbourhood of 8μ and a strong one at about 21μ. Upto 8μ, the absorption of fused quartz follows very closely that of crystalline quartz, except that the peaks are broader (Drummond, 1936). Also, the Raman spectrum of fused quartz exhibits a great similarity to that of crystalline quartz, the lines in the latter being replaced by broad bands in the former (Gross and Romanova, 1929; Kujumzelis, 1935). These show that the infra-red dispersion wavelength λ_2 of vitreous silica is not less than 8μ. Using a value of $\lambda_2 = 8\mu$ and 12μ, it has been calculated that its contribution to dn/dt over the range of wavelengths we are interested in is extremely small compared with that of the ultra-violet frequency and that the contribution progresssively diminishes as λ_2 is taken further away in the infra-red. One

need not therefore be disturbed at the non-occurrence of λ_3 explicitly in the dispersion formula.

Eq. (1) may be put in the form

$$n^2 = C + a_1\lambda_1^2\lambda^2/(\lambda^2 - \lambda_1^2) - K\lambda^2 \qquad (2)$$

where $C = 1{\cdot}36112$, $a_1\lambda_1^2 = 0{\cdot}74655$, $\lambda_1 = 0{\cdot}107044$, $K = 0{\cdot}01350$.

Differentiating (2) with respect to t, and putting $da/dt = -\gamma a$,

$$\frac{dn}{dt} = -\frac{\gamma}{2n}\frac{a_1\lambda_1^2\lambda^2}{(\lambda^2 - \lambda_1^2)} + \frac{1}{n}\frac{a_1\lambda_1^2\lambda^4}{(\lambda^2 - \lambda_1^2)^2}\chi + \frac{1}{2n}\frac{dC}{dt} \qquad (3)$$

where χ and γ have the same significance as in Part I, *viz.*, $\chi = (1/\lambda_1)(d\lambda_1/dt)$ and γ is the coefficient of cubical expansion. The only unknown quantities in the right-hand side of (3) are χ and dC/dt, which we may denote by β.

Measurements of dn/dt for fused silica at a mean temperature of 60° have been made by Martens (1904) for a series of wavelengths from 1850 Å.U. to 6000 Å.U. Using any two measurements, χ and β can be calculated and then the values of dn/dt for a series of wavelengths can be calculated. In this way, the continuous curve in Fig. 1 has been plotted showing

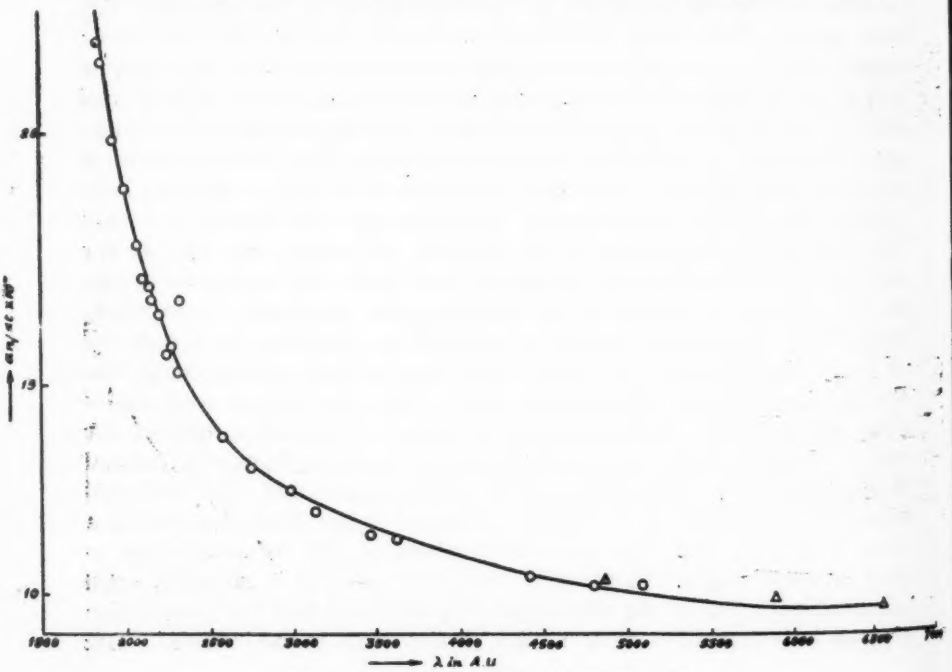

FIG. 1. Variation of dn/dt with wavelength

how dn/dt would vary with wavelength according to theory. The values used for χ and β were $\chi = 24{\cdot}77 \times 10^{-6}$ and $\beta = -10{\cdot}8 \times 10^{-6}$. The circles in Fig. 1 represent the experimental data of Martens (*loc. cit.*). The triangles represent the data of Tilton and Tool (1929). It will be seen that the theoretical curve fits the data well over the whole range of wavelengths.

3. Calculation of the Course of the Refractive Index-Temperature Curve

As in the case of diamond, one may attempt to compare the value of χ for the dispersion frequency with that for other characteristic frequencies. As already mentioned, the Raman spectrum of fused quartz consists of broad bands but in general these bands are in the same positions as the sharp lines in the Raman spectrum of crystalline quartz. For α-quartz, the sharp and intense line at 465 cm.$^{-1}$ stands out prominently in the Raman spectrum. The variation of the frequency of this line with temperature has been studied by Nedungadi (1940) from $-$ 180° upto 500° C. From his data, χ at 60° C. has been calculated to be $3{\cdot}2 \times 10^{-5}$. It is seen that this is of the same order as the value of χ for the dispersion frequency of fused quartz. In fact, the latter is 77% of the former.

One may attempt an extrapolation and assume that this relation between the χ's of the two frequencies is true at other temperatures, *i.e.*, that the proportionate change in frequency of the 1070 Å.U. band of fused quartz is 0·77 times that of the 465 cm.$^{-1}$ line in crystalline quartz. Then, it is possible to calculate the variation of refractive index with temperature over a range of temperatures, using (3). Here, γ is known at various temperatures and χ can be calculated from the above assumption. For dC/dt, some further consideration is necessary. As mentioned in Part I, the term C arises from the constant contribution to refraction of frequencies in the very remote ultra-violet. dC/dt thus arises from the variation in the number of centres and frequency in this term. It may be shown that the contribution to dn/dt due to a dispersion frequency at wavelength λ_ν where $\lambda_\nu << \lambda$ is $(a_\nu \lambda_\nu^2/n)(\chi_\nu - \gamma/2)$. Since dC/dt is negative, it follows that χ_ν is less than $\gamma/2$ *i.e.*, less than $0{\cdot}6 \times 10^{-6}$ at 60° C. Thus χ_ν is less than 2% of the value of χ for the 1070 Å.U. dispersion frequency. This is not unexpected for these remote ultra-violet frequencies arise from transitions of the inner electrons and are not likely to change with temperature. In calculating dC/dt therefore χ_ν was put equal to zero and dC/dt was taken to vary as γ.

If Δn is the change in refractive index for a change of temperature Δt, then from (3) one has

$$\Delta n = -\frac{1}{2n} \cdot \frac{a_1 \lambda_1^2 \lambda^2}{(\lambda^2 - \lambda_1^2)} \cdot \frac{\Delta V}{V} + \frac{1}{n} \cdot \frac{a_1 \lambda_1^2 \lambda^4}{(\lambda^2 - \lambda_1^2)^2} \cdot \frac{\Delta \bar{\nu}}{\bar{\nu}} + \frac{1}{2n} \frac{dC}{dt} \cdot \Delta t \quad (4)$$

Δn was calculated successively between the temperatures – 150°, 0°, 150°, 300° and 450°. $\Delta V/V$ was calculated from the data on thermal expansion. $\Delta \bar{\nu}/\bar{\nu}$ was taken to be 0·77 times the corresponding value for the Raman line 465 cm.$^{-1}$, which was determined from Nedungadi's data (*loc. cit.*). Since the accuracy of these data was only 1 cm.$^{-1}$, a smooth curve was drawn through them and the change in the wave-number determined from the curve. The change from the value at 0° to various temperatures found in this way were: for – 150°, – 1·9 cm.$^{-1}$; 150°, 2·5 cm.$^{-1}$; 300°, 5·3 cm.$^{-1}$;

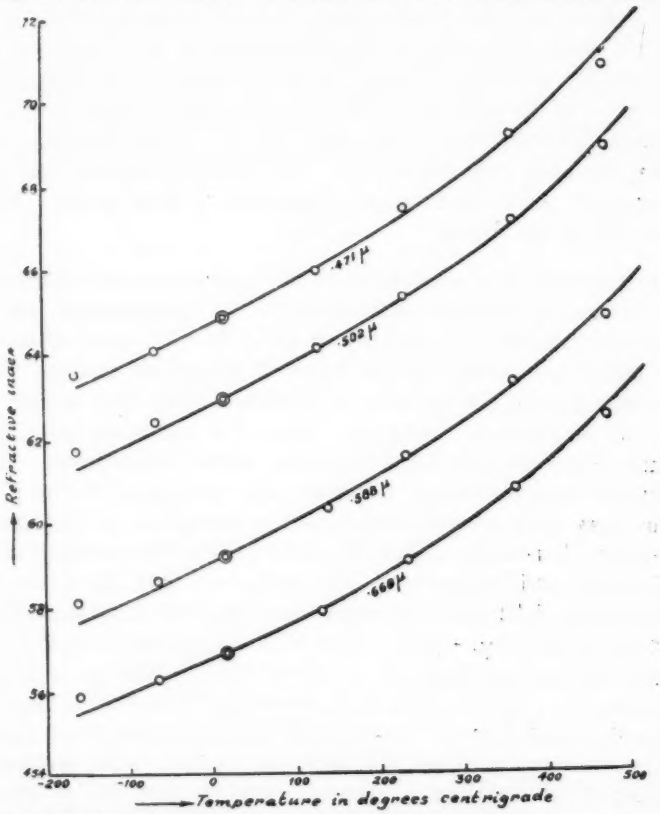

FIG. 2. Refractive index-temperature curves for four wavelengths. The continuous curves are from theory and the circles represent the experimental data.

450°, 8·7 cm.$^{-1}$ The last term was calculated with the assumption just mentioned. In this way, refractive index-temperature curves have been computed and plotted as continuous curves in Fig. 2 for four wavelengths. Experimental data for these are available from the work of Rinne (1914) computed to absolute indices by Sosman (*loc. cit.*). These are shown by circles in Fig. 2. The theoretical curves have in every case been made to pass through the measured value at 18° C. It will be seen that the theory fits the data for higher temperatures upto 500° C. Below 0° C., however, theory gives systematically a lower value than experiment. The discrepancy may be due to the fact that the dispersion frequency varies less in proportion to the infra-red frequency than the ratio 0·77 at these temperatures. It may be mentioned that the error may also be partly due to the fact that Nedungadi's data do not include any measurements in between −190° and 0° C.

In conclusion, I wish to thank Prof. Sir C. V. Raman for the encouragement he gave me during the investigation.

Summary

The theory outlined in Part I of these series has been applied to calculate the thermal variation of refractive index of fused silica. It is found that the theory can account quantitatively for the experimental values of dn/dt over the range of wavelengths from 1850 Å.U. to 6000 Å.U. Using the fact that the frequencies of vitreous silica are practically the same as those of crystalline quartz, the variation of the refractive index with temperature from −130° C. to 500° C. has been calculated and found to fit well with the experimental data.

Reference

1. Coode Adams .. *Proc. Roy. Soc. A.*, 1928, **117**, 209; **121**, 476.
2. Drummond .. *Ibid.*, 1936, **153**, 378.
3. Gross and Romanova .. *Zeits. f. Phys.*, 1929, **55**, 744.
4. Kujumzelis .. *Ibid.*, 1935, **97**, 561; **100**, 221.
5. Martens .. *Ibid.*, 1904, **6**, 308.
6. —— and Micheli .. *Ibid.*, 1904, **6**, 311.
7. Nedungadi, T. M. K. .. *Proc. Ind. Acad. Sci. A.*, 1940, **11**, 86.
8. Radhakrishnan, T. .. *Ibid.*, 1947, this issue.
9. Rinne, F. .. *Neues Jahrb. Min.*, 1914, **39**, 388.
10. Rubens and Nichols .. *Ann. d. Phys u. Chem.*, 1897, **60**, 418.
11. Sosman .. "The Properties of Silica," 1927, Ch. XXIV, 671, *et seq.*
12. Tilton and Tool .. *J. Res. Bur. Stand*, 1929, **3**, 619.
13. Tousey .. *Phys. Rev.*, 1940, **57**, 1060.

THERMO-OPTIC BEHAVIOUR OF SOLIDS

III. Fluorspar

By G. N. Ramachandran

(From the Department of Physics, Indian Institute of Science, Bangalore)

Received March 6, 1947

(Communicated by Sir C. V. Raman, Kt., F.R.S., N.L.)

1. Introduction

In Parts I and II of these series (Ramachandran, 1947), a general theory has been developed for the variation of refractive index of solids with temperature and has been applied to the cases of diamond and vitreous silica. As shown in these papers, the temperature variation of refractive index (dn/dt) can be supposed to consist of two parts, one due to the change in density of the solid and the other due to the changes in the dispersion frequencies, the former being negative and the latter positive, in general. The thermal expansion of both diamond and fused quartz is very small, so that dn/dt for these is positive over the whole spectrum from the far ultra-violet to the red. Fluorspar, on the other hand, has an appreciable thermal expansion and exhibits a negative dn/dt throughout this region. The value is about -5×10^{-6} at 1850 Å.U., which increases numerically to about -12×10^{-6} at 6000 Å.U. (Micheli, 1902) and then again diminishes to about -9×10^{-6} at $6{\cdot}5\mu$ (Liebreich, 1911). It will be interesting to see how far the theory can explain these variations.

The dispersion of fluorspar has been studied by various workers, and a number of dispersion formulæ have been suggested (Jaffé, 1928). The following formula given in the *International Critical Tables*, Vol. VII, p. 12, is said to fit the experimental data from $0{\cdot}185\mu$ to $9{\cdot}4\mu$:

$$n^2 = 6{\cdot}09104 + \frac{0{\cdot}00612093}{\lambda^2 - 0{\cdot}008884} + \frac{5099{\cdot}15}{\lambda^2 - 1258{\cdot}47} \qquad (1)$$

This makes use of an ultra-violet frequency at $\lambda 942{\cdot}6$ Å and an infra-red one at $\lambda 35{\cdot}48\mu$. The ultra-violet frequencies of fluorspar have recently been investigated by Tousey (1936) using a technique analogous to that used for the *Reststrahlen* in the infra-red. It is found that there are two absorption bands, a narrow one with a half-width of roughly 100 Å.U. with its centre at $\lambda 1115$ Å.U. and a stronger and more diffuse band at wave-lengths shorter than 1060 Å.U. and having its maximum at about 900 Å.U. or slightly shorter wave-lengths. In view of Tousey's observations, it will be seen that the above formula (1) can at best only be an

approximation. In fact, it is found that below 1850 Å.U., the formula progressively departs more and more from the experimental values of refractive index as one goes into the ultra-violet. The transmission limit of fluorspar is about 1250 Å.U. and refractive index data down to 1311 Å.U. are available from the work of Handke reported by Martens (1923) in the Landolt-Bornstein Tables. The author has been able to fit these data as well as the data in the visible by a single formula of the form

$$n^2 = C + \sum_1^3 A_r\lambda^2/(\lambda^2 - \lambda_r^2) \qquad (2)$$

with two ultra-violet frequencies at λ 1115 Å.U. and 820 Å.U. and an infra-red frequency at λ 35·48 μ. In fact, a formula of the type

$$(n^2 - 1) = \sum_1^4 A_r\lambda^2/(\lambda^2 - \lambda_r^2) \qquad (3)$$

can also be derived having four dispersion frequencies at λ 450 Å, 888 Å, 1115 Å and 35·48 μ. Details of these will be given in later sections.

The question now arises as to which of these formulæ has to be used for calculating *dn/dt*. It will be evident that as long as a certain formula fits the data for refractive index in the range of wave-lengths in which one is interested, then the theory developed in Part I can be used with that formula for that same range. Consequently, formula (1) has been used for the purpose, which has the advantage of simplicity. It is found that it explains quite well the variations in *dn/dt* described earlier. Later, formulæ (2) and (3) have been applied, and they lead to certain interesting results. It is found that the extreme ultra-violet frequency at λ 450 Å does not vary with temperature, the one at λ 888 Å varies only slightly, while the one at λ 1115 Å varies much more with temperature.

2. Dispersion Formulæ for Fluorspar

Formula (1) mentioned in the previous section can be put in the form:

$$\text{F I: } n^2 = 1{\cdot}35020 + \frac{0{\cdot}68898\,\lambda^2}{\lambda^2 - 0{\cdot}008884} + \frac{4{\cdot}05186\,\lambda^2}{\lambda^2 - 1258{\cdot}47} \qquad (4)$$

Two new formulæ have been developed by the author of the types (2) and (3). They are:

$$\text{F II: } n^2 = 1{\cdot}25910 + \frac{0{\cdot}61667\,\lambda^2}{\lambda^2 - 0{\cdot}0067240} + \frac{0{\cdot}16404\,\lambda^2}{\lambda^2 - 0{\cdot}012432} + \frac{4{\cdot}05186\,\lambda^2}{\lambda^2 - 1258{\cdot}47} \qquad (5)$$

$$\text{F III: } n^2 - 1 = \frac{0{\cdot}45848\,\lambda^2}{\lambda^2 - 0{\cdot}0020250} + \frac{0{\cdot}42824\,\lambda^2}{\lambda^2 - 0{\cdot}0078925} + \frac{0{\cdot}15297\,\lambda^2}{\lambda^2 - 0{\cdot}012432} + \frac{4{\cdot}05186\,\lambda^2}{\lambda^2 - 1258{\cdot}47} \qquad (6)$$

and are meant to represent the refractive indices n with respect to vacuum at λ, the wave-length in vacuum. In Table I, the difference between the values calculated from the above formulæ and the experimental data are given as the number of units in the fourth decimal place. (In Marten's Table quoted earlier, the refractive indices have been given only to 4 decimal places.) It may be mentioned that F I refers only to refractive indices in air. Making correction for the refractive index of air, the errors are shown in brackets under F I. It will be seen that the error becomes larger and larger as one progresses into the ultra-violet beyond $0{\cdot}185\,\mu$. F II and F III on the other hand fit very well down to $0{\cdot}16\,\mu$ beyond which both show a peculiar type of error. The difference between experiment and theory is first positive, becomes larger and larger, reaching a maximum at about $0{\cdot}145\,\mu$, then diminishes and becomes negative. The author found that no manipulation with the frequencies below λ 1115 Å.U. can improve the fit in this region. In fact, when the experimental dispersion curve is plotted, an anomalous rise in refractive index is found down to about $0{\cdot}145\,\mu$ and then an anomalous fall is found. A similar variation is found in Tousey's reflection curve also (*loc. cit.*). All these suggest that there is an extremely weak absorption band with its centre at about $0{\cdot}134\,\mu$ (at which wave-length the error passes from positive to negative values), which is the cause for the anomalous dispersion in its neighbourhood.

TABLE I

λ_{vac} in microns	n_{vac} exp.	$n_{exp}-n_{th}$		
		FI	FII	FIII
0·76845	1·4313		0	0
0·58947	1·4342	+3 (−1)	0	0
0·394524	1·4427		0	0
0·308314	1·4530		0	0
0·257392	1·4653	+4 (−1)	0	0
0·219527	1·4821		0	0
0·199057	1·4969	+8 (+2)	0	0
0·185477	1·5107	+10	0	0
0·176420	1·5227	+14	0	0
0·164455	1·5438		0	0
0·15692	1·5615		−1	−1
0·15234	1·5751	+46	+1	+1
0·14817	1·5896		+2	+2
0·14363	1·6089	+88	+6	+5
0·13940	1·6305		+4	+3
0·13536	1·6565		+1	+1
0·13192	1·6844	+237	−3	−2
0·13111	1·6921		−4	−3

3. Calculation of dn/dt for Various Wave-lengths

A. Using F I.—As was mentioned earlier, formula F I represents the refractive index sufficiently well for wave-lengths larger than 1850 Å.U. One may therefore calculate dn/dt from it in the same manner as was done for fused quartz. If one writes

$$n^2 = C + \sum_r a_r \lambda^2_r \lambda^2/(\lambda^2 - \lambda_r^2), \tag{7}$$

then

$$\frac{dn}{dt} = \frac{\beta}{2n} - \frac{\gamma(n^2 - C)}{2n} + \frac{1}{n}\sum_r \frac{a_r \lambda_r^2 \lambda^4 \chi_r}{(\lambda^2 - \lambda_r^2)^2} \tag{8}$$

where $\beta = (dC/dt)$, $\chi_r = (1/\lambda_r)(d\lambda_r/dt)$ and γ is the coefficient of cubical expansion. The value of χ_3 for the infra-red frequency is available from the unpublished work of D.C. Press carried out in this laboratory on the temperature variation of the principal Raman frequency at 320 cm.$^{-1}$ It is

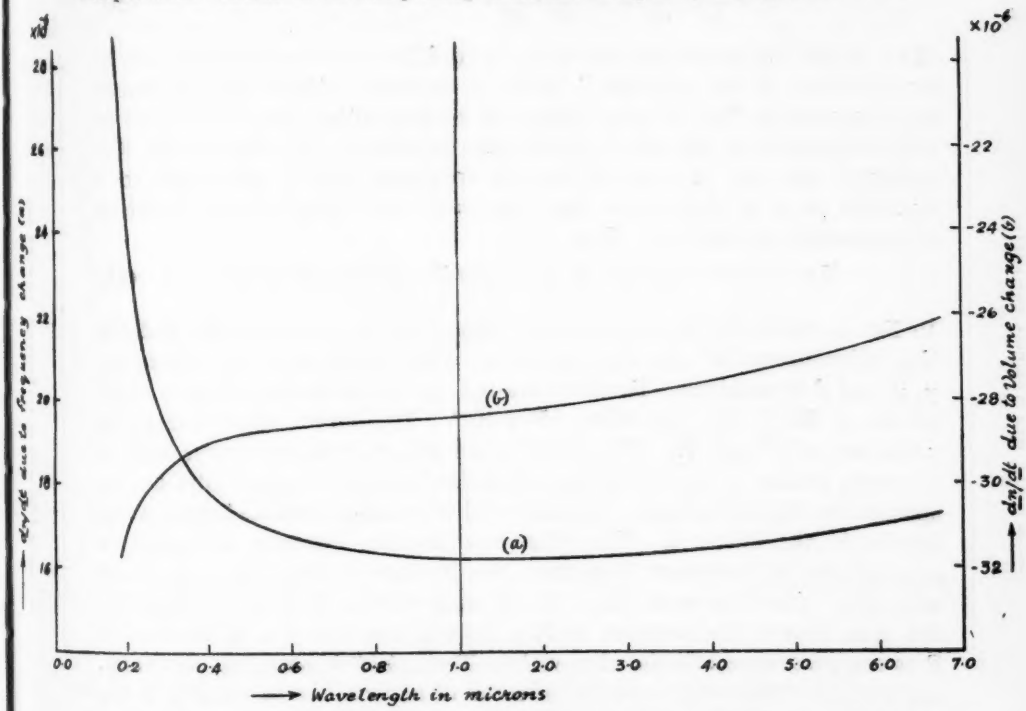

FIG. 1. Curves showing the variation with wavelength of the contributions to dn/dt due to volume and frequency changes. The abscissæ have been reduced five-fold after 1 μ to facilitate the whole range from 0·2 μ to 7 μ being shown in the same diagram. The scale of the ordinates for both the curves is the same, but the origins have been shifted.

found that the contribution to dn/dt due to the change in the infra-red frequency is negligible for the visible and ultra-violet regions of the spectrum, being less than 1% at $0{\cdot}8\,\mu$ and less at shorter wave-lengths.

The calculations were done for 60° C. for which temperature the dn/dt data are all available. γ was obtained from the unpublished work of D C. Press in this laboratory. There are only two unknown quantities, χ_1 and β, which were calculated to have the values

$$\chi_1 = 33{\cdot}1 \times 10^{-6} \text{ and } \beta = -37{\cdot}6 \times 10^{-6} \tag{9}$$

As mentioned earlier, dn/dt can be supposed to be composed of two parts, due respectively to the change in density and change in dispersion frequency, which we may denote by P and X, following the notation in Part I. Thus,

$$\mathrm{P} = \frac{\partial n}{\partial \rho} \cdot \frac{d\rho}{dt}, \quad \mathrm{X} = \frac{\partial n}{\partial \lambda} \cdot \frac{d\lambda}{dt}. \tag{10}$$

Now, in the expression (8) above, the term $\beta/2n$ is the contribution due to the alteration of the constant C, which is negative. Following the reasoning advanced in Part II with respect to vitreous silica, one may conclude that this part is wholly due to the change in volume. In other words, it is assumed that the extreme ultra-violet frequency which gives rise to a constant term in dispersion does not vary with temperature, which is a reasonable assumption. Thus,

$$\mathrm{P} = -\gamma(n^2 - \mathrm{C})/2n + \beta, \quad \mathrm{X} = (1/n) \sum_r a_r \lambda_r^2 \lambda^4 \chi_r / (\lambda^2 - \lambda_r^2)^2 \tag{11}$$

In Fig. 1, these two parts are shown separately by the curves (*a*) and (*b*). The calculations for drawing the curves were made with the values for γ, χ_1 and β given above. For the infra-red, χ_2 was taken from Press's work, which at 60° C. has the value 159×10^{-6}. The curves show interesting variations of P and X. The contribution due to volume change follows a course similar to the refractive index, diminishing (algebraically) as one approaches the ultra-violet frequency and increasing towards longer wave-lengths in the infra-red. The other contribution, however, increases on approaching a dispersion frequency, the increase taking place on either side of it. This is because it is inversely proportional to $(\lambda^2 - \lambda_r^2)^2$, and for the same reason, the increase in X preponderates over the diminution in P as one progresses into the ultra-violet. Thus, *dn/dt increases* on approaching both the ultra-violet and the infra-red dispersion bands. In Fig. 2 the course of the $(dn/dt) - \lambda$ curve is shown, which will illustrate this fact. The continuous curve has been calculated from theory, while the points are the experimental data of Micheli (1902) and Liebreich (1911), the former

being shown by circles and the latter by triangles. It will be seen that the agreement with Micheli's data is remarkably good. Liebreich's data exhibit an appreciable algebraic increase in dn/dt from $0{\cdot}8\mu$ to 2μ and a relatively smaller increase thereafter than indicated by theory. In this region, theory gives systematically lower values, although it agrees with the data at longer wave-lengths. The author is unable to conceive of any reason as to why dn/dt should quickly increase (algebraically) upto 2μ. In fact, as will be seen later in this section, the use of other dispersion formulæ like F II and F III does not alter the theoretical curve sensibly and that the discrepancy is still present. It would appear that the discrepancy between theory and experiment in this region must be attributed to experimental errors, which are likely to be large since dn/dt is only obtained indirectly from the difference in the refractive indices at two temperatures and also since the latter measurements themselves are less accurate than in the visible because no photographic method can be used.

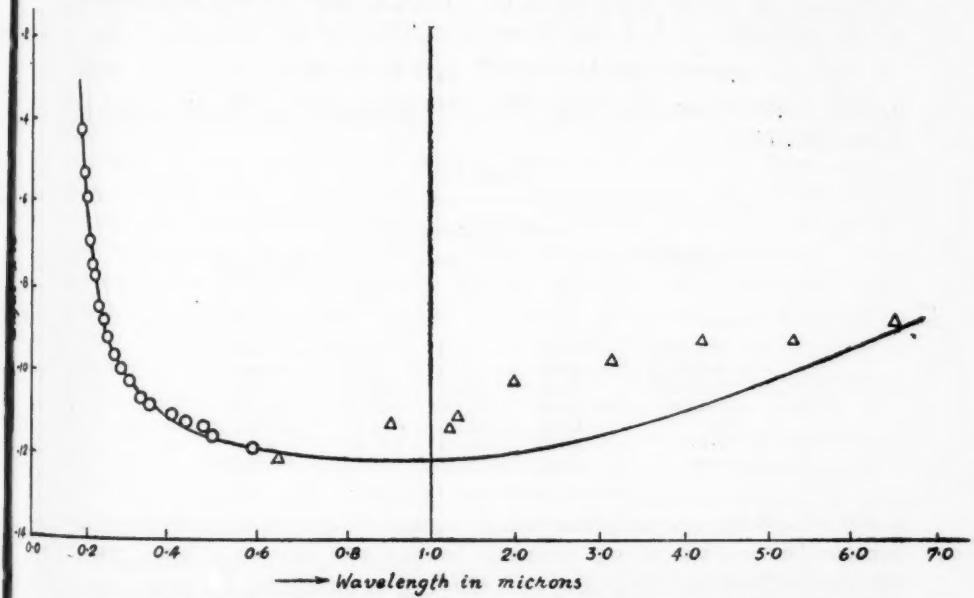

FIG. 2. Variation of dn/dt with wavelength. The circles are the experimental data of Micheli and the triangles those of Liebreich. The scale has been compressed five-fold above $1{\cdot}0\mu$.

B. Using F II and F III.—We have thus seen how a relatively approximate formula like F I is sufficient to explain the variations in dn/dt. We shall now apply the new formula F II, which is also of the form (7), so

that dn/dt is given by (8). Now, there are two ultra-violet frequencies at λ 1115 Å.U. and 820 Å.U. For convenience, we shall assume that both of them vary with temperature to the same extent in proportion to their frequency, in other words that both have the same value of χ. Then, it is found that β and χ have the values:

$$\chi = 33{\cdot}0 \times 10^{-6}, \quad \beta = -37{\cdot}6 \times 10^{-6} \tag{12}$$

The resulting formula fits the data for dn/dt very well. In Table II below, the calculated values of dn/dt for a few wave-lengths from F I, F II and F III are given together with the experimental values. It will be seen that there is little to choose between the three formulæ.

However, F III is interesting because it is of the standard type given by the Ketteler-Helmholtz theory with the constant $C = 1$ in (7). Consequently, dn/dt does not involve an arbitrary constant β, but depends only on the values of χ_r for the dispersion frequencies. Denoting the four frequencies at $\lambda\lambda$ 450 Å.U., 888 Å.U., 1115 Å.U. and 35·47 μ respectively by the subscripts 1, 2, 3 and 4, one finds that the χ_r's have the values:

$$\chi_1 = 0, \quad \chi_2 = 11{\cdot}3 \times 10^{-6}, \quad \chi_3 = 70{\cdot}2 \times 10^{-6} \tag{13}$$

χ_4 was taken to have the value 159×10^{-6} obtained from Press's measurements (*loc. cit.*).

TABLE II

Wavelength in microns	dn/dt calculated from			dn/dt from experiment
	F I	F II	F III	
0·199057	− 6·07	− 5·92	− 5·93	− 5·89
0·257392	− 9·26	− 9·19	− 9·39	− 9·24
0·308314	−10·45	−10·36	−10·44	−10·32
0·58947	−11·84	−11·91	−11·78	−11·93
1·3	−12·23	−12·16	−11·91	−11·21
3·16	−11·63	−11·55	−11·28	− 9·83
6·5	− 9·15	− 9·05	− 8·78	− 8·84

It will be seen the proportionate rate of change of the ultra-violet frequencies becomes less and less as one proceeds further into the ultra-violet. Thus the remote dispersion frequency at λ 450 Å.U. is unaffected by temperature while between the two at λ 888 Å and λ 1115 Å., the latter increases much more than the former. It may be mentioned that the actual numerical values given in (13) can be altered slightly and yet fit the experimental data. However, it will be found that always $\chi_3 > \chi_2 > \chi_1$, the last one being very small.

3. Discussion of the Results

The result just mentioned is what one would expect from other considerations. Of the various ultra-violet frequencies, those having higher frequencies should arise from the deeper levels of the atoms, while those with lower frequencies arise from transitions between the levels of the outer electrons. Since the outer electrons take part principally in the binding of the crystal, a change in temperature would be expected to affect the levels of the outer electrons much more than those of the inner ones.

Another interesting fact emerges when one compares the value of χ for the ultra-violet frequencies with that for the characteristic infra-red frequency of the lattice. It was shown in Parts I and II that these two are of the same order in diamond, and that in fused quartz χ of the dispersion frequency is of the same order as χ of the intense Raman line at 465 $cm.^{-1}$ of α-quartz. For fluorspar, although the temperature variation of the infra-red active lattice frequency has not been studied, data on the Raman frequency at 320 $cm.^{-1}$ (which lies close to the former) are available (Press, *loc. cit.*). If one takes F I or F II, then χ for the ultra-violet frequencies is about 33×10^{-6} which is only about 1/5 of χ for the infra-red, *viz.*, 159×10^{-6}. If we denote by χ_V and χ_R the values of χ for the ultra-violet and infra-red frequencies, then χ_V/χ_R is 78% for diamond and 77% for fused quartz while it is only 21% for fluorspar. Even if one takes F III and considers χ_3, the variation of the frequency at λ 1115 Å.U., then also, χ_3/χ_R is only 45%. Thus, the ultra-violet frequencies vary much less relatively in fluorspar than in diamond and fused quartz when compared with the variation of the lattice frequency of the respective crystals. The interpretation of this difference is not far to seek. Both diamond and quartz are typical covalent solids, in which the binding is essentially produced by the sharing of the outer electrons. One would therefore expect the changes in the binding energy and changes in the electronic states of the outer electrons to correspond closely in these solids. In fluorspar, the binding is not so highly covalent as in diamond or quartz, but is partly electrovalent. It is therefore not surprising that the ultra-violet electronic transitions are relatively less affected by temperature than the infra-red lattice frequency.

One may also consider what happens to χ_V at elevated temperatures. For this, one can make use of the work of Reed (1898) who has determined dn/dt for sodium light for various temperatures above the room temperature. γ can be obtained from the data of Press mentioned earlier. It is assumed that the component of dn/dt produced by change of volume varies in the

same proportion as γ. This means that β is taken to vary as γ, which is true since β is due only to a change in volume, the extreme ultra-violet frequency not altering with temperature. The important values used in the calculation, as well as the values of χ_V (calculated with FI) and χ_R (calculated from Press's data) are shown in Table III.

TABLE III

Temperature °C	$dn/dt \times 10^6$	$\gamma \times 10^6$	$\chi_V \times 10^6$	$\chi_R \times 10^6$
60	−11·9	63·24	33·1	159
100	−12·4	64·17	32·8	131
150	−13·1	65·58	32·7	110
200	−13·7	67·50	33·2	94
250	−14·3	70·35	34·4	90

It will be noticed that χ_V is practically a constant upto 200° C. after which it rises slightly. χ_R on the other hand shows an appreciable decline with rise of tempearture. In both diamond and fused quartz, χ_V increases with temperature. Although the precise reason for the difference in the case of fluorspar is not clear, one may reasonably attribute it to the differences in the nature of binding in the crystal.

I am very grateful to Prof. Sir C. V. Raman for the kind and encouraging interest that he took in this investigation. I am also thankful to Mr. D. C. Press for having kindly made available to me the unpublished results of his studies on fluorspar.

SUMMARY

Making use of the dispersion formula given in the International Critical Tables, with absorption bands at $\lambda\lambda\, 0{\cdot}0942$ and $35{\cdot}48\,\mu$, and using the theory developed in Part I, the course of the variation of dn/dt with wave-length has been satisfactorily explained from $0{\cdot}185$ to $6{\cdot}5\,\mu$. The dispersion formula however fails below $0{\cdot}185\,\mu$, and consequently two new formulæ have been developed holding down to 1300 Å.U., one of which uses dispersion frequencies at $\lambda\lambda\, 0{\cdot}082$, $0{\cdot}1115$ and $35{\cdot}48\,\mu$ together with a non-unity constant in the expression for n^2, while the other is of the Ketteler-Helmholtz type with four frequencies at $\lambda\lambda\, 0{\cdot}045$, $0{\cdot}088$, $0{\cdot}1115$ and $35{\cdot}48\,\mu$. All the formulæ explain the variations of dn/dt, in particular, as to why it increases algebraically as one proceeds both into the ultra-violet and the infra-red. The interesting fact emerges that the extreme ultra-violet frequency at $\lambda\, 0{\cdot}045\,\mu$ does not vary with temperature, while the proportionate variation of the one at $0{\cdot}0888\,\mu$ is much less than that of the

one at 0·1115μ. This result becomes intelligible when one remembers that the deeper levels in the crystal would be less affected by temperature than the low-lying ones. Even the last one, although it is of the same order, is only one half of the proportionate variation of the infra-red lattice frequency. It is also found that the rate of variation of the ultra-violet frequencies is constant at different temperatures. In these respects, fluorspar differs from diamond and vitreous silica. The difference has been attributed to the fact that the binding in fluorspar is not purely covalent, but is also partly electrovalent.

References

1. Jaffé, G. .. *Handb. d. Exp. Phys.*, 1928, **19**, 176.
2. Liebreich, E. .. *Verh. Deutsch. Phys. Ges.*, 1911, **9**, 1.
3. Martens, F. F. .. *Landolt Börnstein Tables* V Edn., Hauptwerke, 1923, Vol. II, 911.
4. Micheli, F. J. .. *Ann. d. Phys.*, 1902, **7**, 772.
5. Ramachandran, G. N. .. *Proc. Ind. Acad. Sci.*, A, 1947, this issue.
6. Reed .. *Ann. d. Phys. u. Chem.*, 1898, **65**, 734.
7. Tousey, R. .. *Phys. Rev.*, 1936, **50**, 1057.

86-47 Printed at The Bangalore Press, Bangalore City by G. Srinivasa Rao, Superintendent
and Published by The Indian Academy of Sciences, Bangalore

Description of Plate X, Vol. XXV, A, 1947

1. Spectrum (*a*) is taken on E_1 Hilger quartz spectrograph using Kodak Superpanchro press P-1200' plate.

2. Spectrum (*b*) is taken on Medium Hilger quartz spectrograph using Kodak Process Regular B-20' plate.

ERRATA

Vol. XXV, A, No. 2, February 1947

Page 133, First line in foot note, *for* $\{[\sigma_g^2, \Pi_u^4, \Pi_g^3\ {}^2\Pi_{g3/2}]\ \sigma_g^2\}$
read $\{[\sigma_g^2, \pi_u^4, \pi_g^3 \cdot {}^2\Pi_{g3/2}]\ \sigma_g^2\}$

Page 134, Fourth line, *for* $1_g\ ({}^3\Sigma_g^+)$ *read* $1_g\ ({}^3\Sigma_g^-)$

Page 137, 23rd line, *for* $O_g^+\ ({}^3\Sigma_g)$ *read* $O_g^+\ ({}^3\Sigma^-)$

Page 149, 28th line, *for* 51583 *read* 51528